FOLD GEOMETRY AND CONSTITUTIVE BEHAVIOUR

B.E. HOBBS[1], H-B. MÜHLHAUS[2], A. ORD[2], Y. ZHANG[2] AND L. MORESI[2]

Australian Geodynamics Cooperative Research Centre,
CSIRO Exploration and Mining,

[1] Private Mail Bag 5, Wembley, 6913, Australia
[2] P.O. Box 437, Nedlands, 6009, Australia

Hobbs, B.E. , Mühlhaus, H-B., Ord, A., Zhang, Y. and Moresi, L. 2000. Fold Geometry and Constitutive Behaviour. In: Stress, Strain and Structure, A volume in honour of W D Means. Eds: M.W. Jessell and J.L.Urai. Volume 2, Journal of the Virtual Explorer.
ISSN 1441-8126 (Print). ISSN 1441-8134 (CD-ROM).
ISSN 1441-8126 (On-line at www.virtualexplorer.com.au/VEjournal/Volume2).

1. MOTIVATION FOR THIS PAPER

1.1 The Issue

An ideal to which structural geologists aspire is to be able to infer the physical and chemical conditions of deformation and the constitutive behaviour of deformed rocks by examining the intricate geometry of the deformation. Thus, one would like to be able to say something about the temperature, the pressure, the strain distribution, the volume change distribution, the deformation rate tensor, the stress tensor, the fluid pressure, the fluid flux and rates of chemical reactions relative to the deformation rates and fluid flux rates by examining the geometry of the deformation. In addition, one would like to say if the material was behaving as a viscous material (perhaps even specify the power law exponent linking stress to deformation rate), or perhaps as elastoviscous or elastoplastic materials or as materials with even more complicated constitutive behaviour.

In this paper we select *folding* as an important and spectacular geological structure and explore recent progress towards the above ideal. Our emphasis is upon examining various (relatively simple) constitutive behaviours and exploring the fold geometries that arise from these behaviours. For simplicity, we restrict the discussion to only single layer folded systems.

The plan of this paper is as follows: In Section 1 we expand upon the issue involved here and point out that although simple theoretical rheological arguments predict single wavelength, strictly periodic fold trains, in reality in Nature we observe aperiodic or irregular fold geometries. We ask: Why is this so? In Section 2 we elaborate briefly on what we mean by the terms *elasticity*, *viscosity* and *plasticity* and introduce the concept of *time scales* for various deformation responses. In Section 3 we consider deformation of purely elastic or purely viscous single layer materials and follow in Section 4 with a consideration of elastoviscous materials where we show that two wavelength systems can occur. In Section 5 we consider folding of more exotic materials which couple elasticity and viscosity but with some form of non-linear behaviour also involved: fold systems with elements of fractal geometry and chaotic dynamics develop under such situations. Finally, we consider some recent developments involving the evolution of microstructures and microfabrics during folding or other deformations and the feedback such fabric evolution has on constitutive behaviour and hence upon full evolution. Section 6 summarises the paper.

The classical treatments of buckling of single layers embedded in another medium originated with Biot (1937, 1957, 1959, 1961, 1963, 1965), although identical developments were made by Ramberg (1963). These classical treatments are two dimensional, linear theories. The term *linear* means that only linear constitutive laws are examined (either elastic or linearly viscous but not power law viscous, plastic, or elastic-viscous behaviour); geometrical non-linearities related to large deflections or curvatures are excluded. The common result of all such treatments, no matter whether the layer or the embedding materials be elastic or linearly-viscous is that just one particular wavelength (the Biot dominant wavelength) is amplified with an exponential growth law. Thus, strictly periodic fold geometries always result from the classical theories no matter what initial geometry or initial deviations from the ideal planar state exist.

The problem is usually set up as shown in Figure 1.

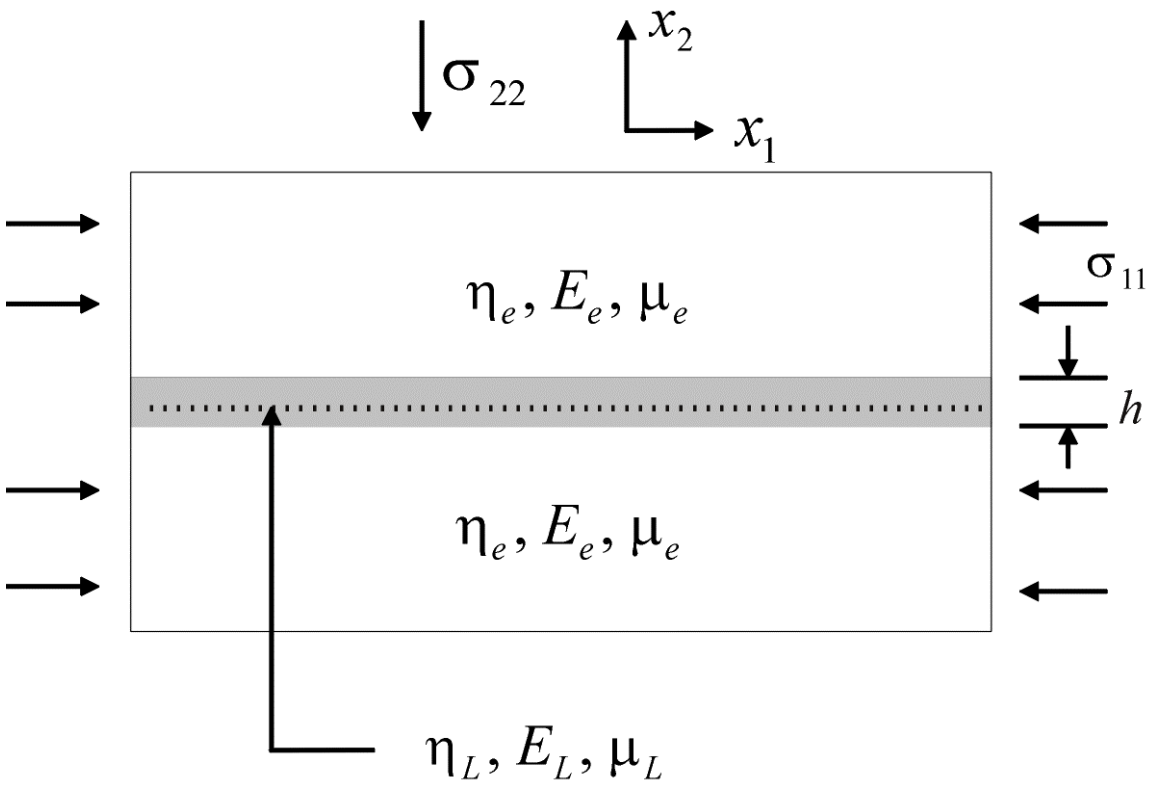

Figure 1: The problem to be considered in this paper. A single layer of thickness, h, and with Young's Modulus, E_L, elastic shear modulus, μ_L, and viscosity, η_L, is embedded in a medium with Young's Modulus, E_e, elastic shear modulus, μ_e and viscosity, η_e. The assembly is shortened in the x_1 direction either by an imposed stress, σ_{ij}, or by an imposed strain rate. The question is: What is the geometry of folds that form in the layer and how is this geometry influenced by the constitutive behaviour?

A single thin layer of thickness, h, is embedded in a medium and the whole assembly is subjected to either constant velocity or constant stress boundary conditions in the direction parallel to the initial orientation of the layer. Treagus (1973) has considered the situation where the shortening direction is oblique to the initial orientation of the layer. The constitutive parameters for the layer are the Young's Modulus, E_L, the elastic shear modulus, μ_L, and the viscosity, η_L. Similarly, for the embedding medium these parameters are E_e, μ_e and η_e respectively. The contrast in these parameters between layer and the embedding medium is known as the *competency contrast* (R), following Willis (1893) who proposed that competency was a measure of how well a material could support externally imposed stresses.

R_{elast} is the competency contrast in the elastic parameters whilst R_{visc} is the competency contrast in the viscosities. Notice that R_{elast} can represent the contrast in either the Young's Modulus or the shear modulus; these two contrasts are equal for a common Poisson's Ratio for both the layer and the embedding medium.

As an example, for a linear viscous constitutive law, the Biot dominant wavelength is given by

$$\lambda = 2\pi h \sqrt[3]{\frac{\eta_L}{6\eta_e}} \qquad (1)$$

And the growth coefficient corresponding to this wavelength for constant stress boundary conditions is

$$\omega = \frac{\sigma_{11} - \sigma_{22}}{6\eta_L} \left(\frac{2\pi}{\lambda}\right) \qquad (2)$$

where σ_{11}, σ_{22}, are the stresses shown in Figure 1; see Mühlhaus *et al*. (1998).

However, natural folds are rarely, if ever, strictly periodic; that is they are rarely characterised by a single dominant wavelength. A clear example here is the ubiquitous existence in Nature of parasitic folds; here such geometries are characterised by two dominant wavelengths, a situation which is never predicted within the classical theories of Biot and Ramberg.

Moreover, even greater complexity in fold geometry is common, and some examples are shown in Figure 2. Strict periodicity with respect to wavelengths is very rare and we explore this complexity in a little more detail in an example below.

a)

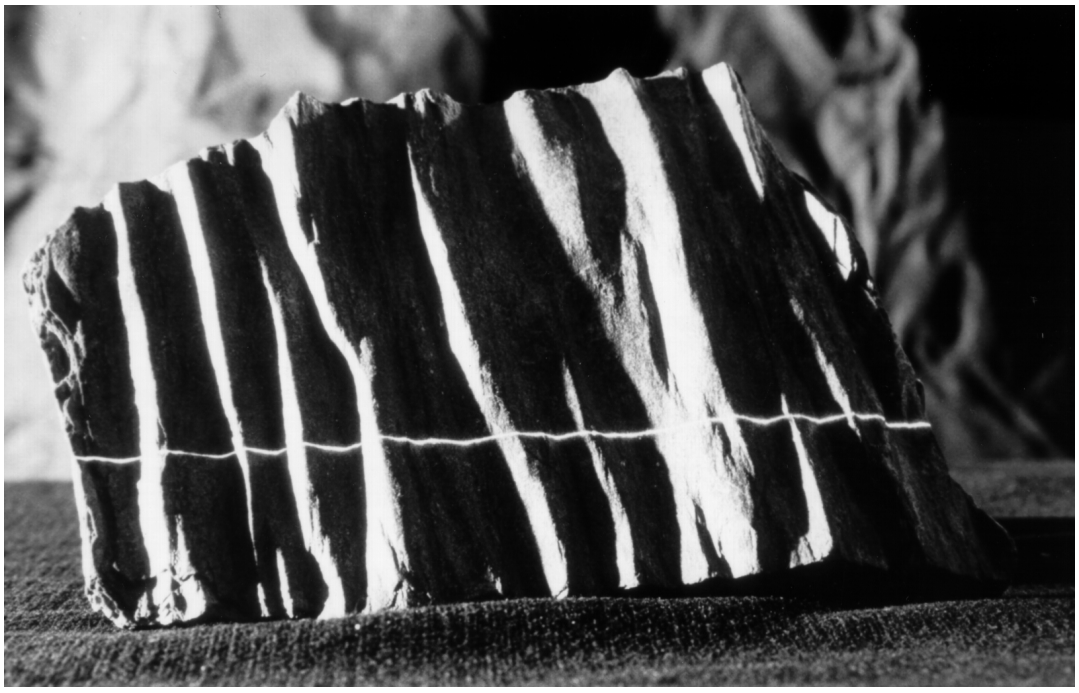

b)

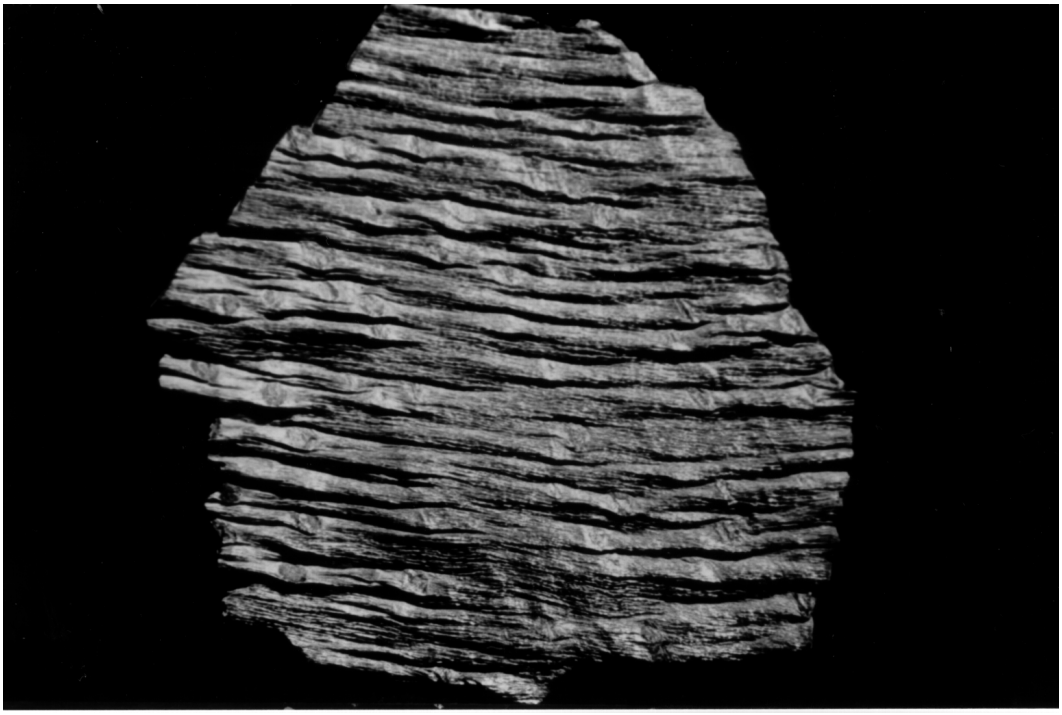

c)

Figure 2: Examples of natural fold geometries. In (a) a thin planar laser beam is shown intersecting the surface of a folded layer. A series of such intersections is used to construct Figure 3.

Figure 3 shows a series of adjacent scans across the surface of a folded layer from the natural fold system shown in Figure 2(a). The scans were made using a thin planar laser beam and the resultant image, which represents the intersection of the planar beam with the folded surface, was captured using a video camera into a frame grabber.

Erratic behaviour in time series has been analysed for a variety of non-linear dynamic systems; here we are concerned with spatially erratic behaviour. Techniques for analysis of spatiotemporal chaos have been described by, for example, Mayer-Kress and Kaneko (1989) for coupled map lattices. We construct an "attractor" (see Figure 4) for the spatial pattern shown in Figure 3 in the same way that Packard *et al*. (1980, see also Takens, 1981, Crutchfield *et al*., 1986) obtained the attractor for a time series. We explore whether the evolution of one component of a system is determined by its interaction with other components, and reconstruct an 'equivalent' state space by examining the measured values at fixed space (rather than fixed time) delays with respect to a single component as though these space delays were new dimensions in this 'equivalent' state space. In this instance, the component of the system is the displacement of a given point on the profile of the fold relative to a datum. We are then able to examine the dimension (Figure 5) of this spatial attractor within different embedding dimensions, and infer the dimension of the system (for a succinct review, see Ruelle, 1990). The dimension of the system is representative of the number of degrees of freedom of the system, and therefore of the number of independent, non-linear differential equations required to describe the system.

Details of the procedure whereby Figure 4 is constructed may be found in Ord (1992). Again, following the procedures spelt out in Ord (1992), Figure 5 indicates that the "spatial attractor" shown in Figure 4 has a fractal dimension of 2.3. Thus, the attractor of Figure 4 is fractal; a periodic fold system would have given a plot with dimension exactly two.

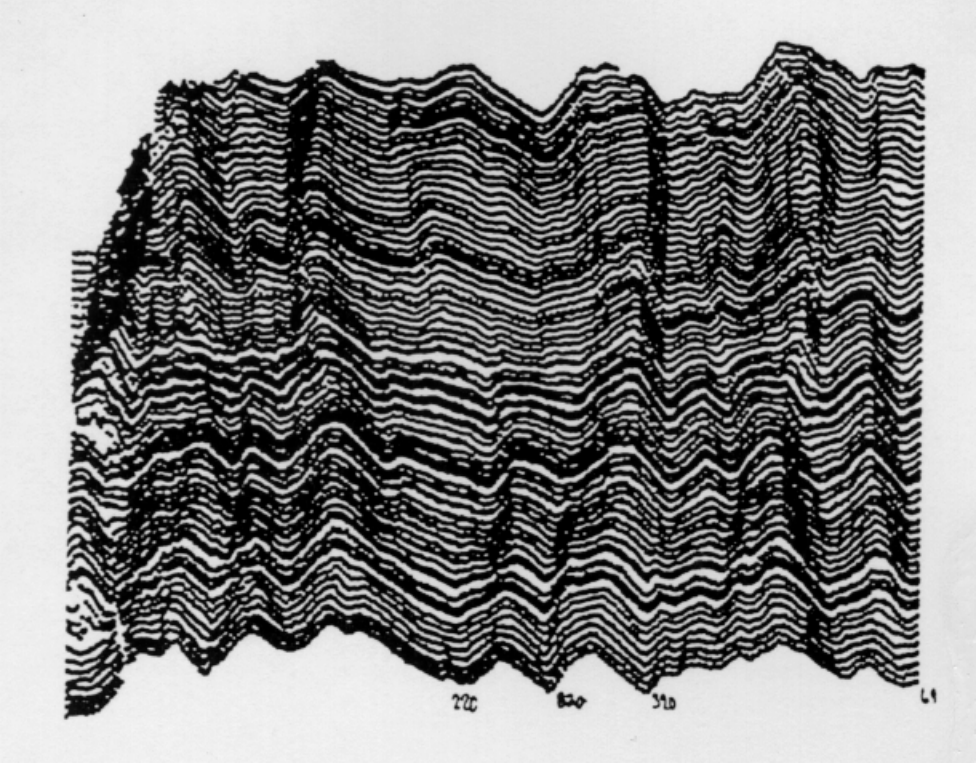

Figure 3: A series of laser scans across the folded surface shown in Figure 2(a).

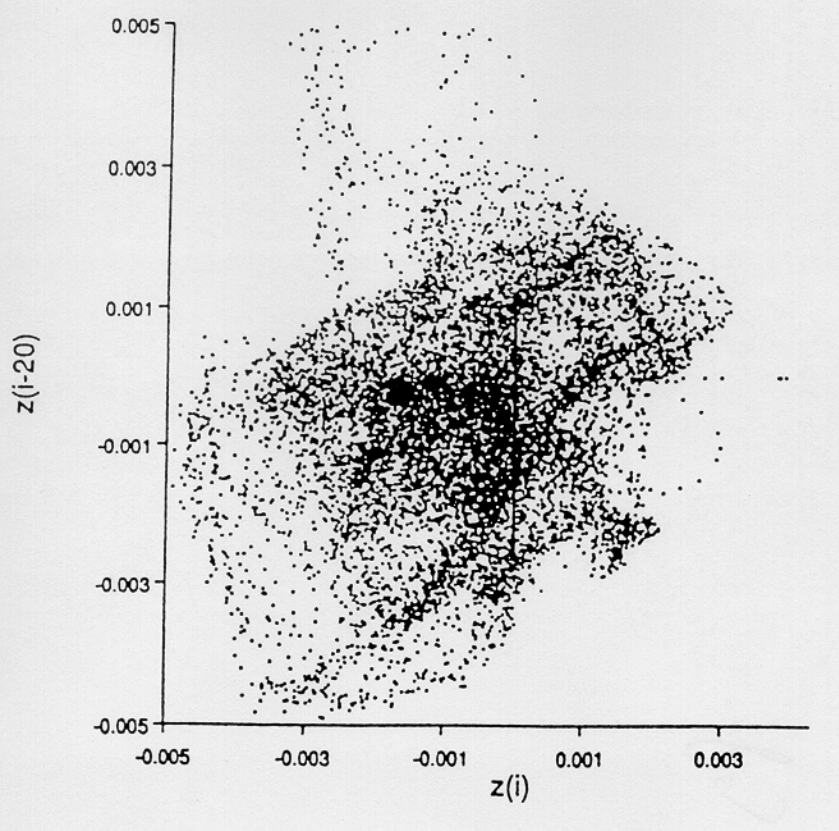

Figure 4: A "spatial attractor" for the series of profiles shown in Figure 3. See text for method of construction.

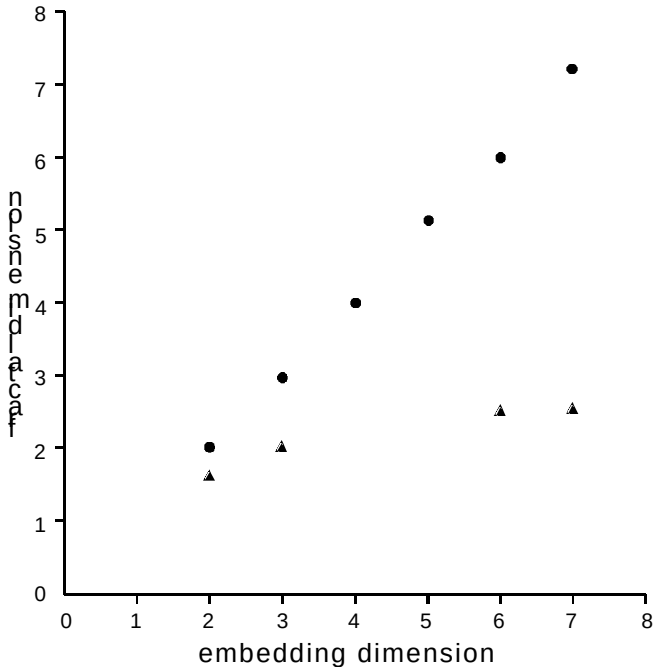

Figure 5: Plots of Fractal Dimension against Embedding Dimension for a random distribution (full circles) and for the "spatial attractor" shown in Figure 4 (triangles).

Even in these situations where an approximation to periodicity is developed, a question remains: Is the wavelength we observe in such situations really the Biot dominant wavelength, given for the linear viscous material as expression (1)? Or does mechanical behaviour more complicated than linearly elastic or viscous lead to wavelengths that differ from the Biot Wavelength?

For instance, many authors would propose that real geological materials behave as viscous materials with a non-linear, power law relationship between the magnitudes of strain rate and stress. The question therefore arises: Do these non-linear viscous materials also develop fold geometries in which the dominant wavelength is given by (1)? Of course, even asking this question raises the question of how we adequately define the viscosity for such a non-linear material. These issues are addressed in Section 3.

The aim of this paper is to explore the various issues and questions raised above. In part, the paper is a review of existing work although in the grand tradition of Win Means, to whom this paper is dedicated, the approach is to be didactic and to extract from the now diverse literature on the subject, those pertinent relationships and results that would enable us to go into the field and say something constructive about the rheology of the folded rocks we see from the geometry that is portrayed. Where necessary, we illustrate the conclusions made with new theory and computer simulations. We make no attempt to be comprehensive in our review.

1.2 The Problem

The observed non-periodicity of fold systems can have at least two explanations:

(i) Perhaps Biot-Ramberg type arguments concerning the amplification of a dominant wavelength need to be moderated by introducing a strong influence upon final fold geometry of initial geometrical or material imperfections. This is the argument proposed by Cobbold, 1975, 1977; Williams *et al*., 1978; Abbasi and Mancktelow, 1990, 1992; Mancktelow and Abbasi, 1992; Mancktelow, 1999. In particular, the results of Mancktelow, 1999, would suggest that at proposed geological strain rates of 10^{-14} s^{-1}, initial geometrical irregularities always control the final fold geometry and Biot/Ramberg buckling processes play a relatively minor role.

(ii) Perhaps buckling behaviour is indeed the dominant behaviour but the controlling processes are more complicated than is proposed in the classical treatments of the problem. The basic tenet of such approaches is that non-linearities in the constitutive behaviour such as non-linear elasticity, coupling between elastic and viscous behaviour, strain- or strain rate softening or microstructural dependent yield or flow stresses lead to non-periodic geometries. We explore such developments in this area in Sections 4 and 5.

An important point to emphasize here is that if explanation (i) is important, then homogeneous deformation and the passive amplification of initial geometrical irregularities probably play a critical role in the development of folds we see in Nature. In extreme cases, the growth rate of dynamic folding is very low so that homogeneous deformation dominates all or much of the buckling histories and the end product of folding is essentially the passive

amplification of the initial geometrical perturbations. During such folding processes, fold hinges are fixed at the inception of deformation and do not migrate along the layer with respect to material particles as the fold geometry evolves. An example of such a process is shown in Figure 6(b). Here the final geometry clearly represents the passive amplification of the initial irregular geometry of Figure 6(a). In other cases, the growth rate of dynamic folding may be able to dominate in later folding stages after significant initial homogeneous shortening, and hence folding can switch from the passive growth mode to the dynamic amplification mode. However, the limb dips of geometrical perturbations may have already reached finite amplitude fields (e.g. > 10°) during the stages where homogeneous deformation and passive amplification dominate. Therefore dynamic folding in later stages of deformation may just follow the pattern of already amplified initial perturbations, so that again fold hinges do not migrate along the layer. These are the type of processes that are predicted by the classical Biot/Ramberg theories at very low competence contrasts (say R = 10 or below). One should emphasize that Mancktelow (1999) has reported this kind of behaviour for competency contrasts as large as 200 at strain rates of 10^{-14} s^{-1}.

On the other hand, if Biot type buckling processes are relevant, then although there may be a period of initial homogeneous layer parallel shortening, a dominant wavelength will soon be selected and grow exponentially. As a result, a single wavelength, unrelated to the geometry of initial geometrical irregularities but determined by layer thickness and competency contrast, is developed ultimately.

An example is shown in Figure 6(c). The model starts from the same initial geometry (Figure 6(a)) as the previous example (Figure 6(b)) but in contrast a regular fold train with a dominant wavelength is ultimately developed; note that the change in folding is purely due to the change in strain rate, the effect of which on folding will be discussed subsequently. Here there must be some migration of fold hinges along the layer relative to the positions of material particles but such migration only occurs during early folding stages while limb dips are still low. Notice that the positions of initial irregularities here play no part in controlling the positions of fold hinges (Figure 6(c)). Again, one should emphasize that Zhang *et al.* (1996) have reported such behavior for competency contrasts as low as 20 so there is a problem in reconciling the results of Zhang *et al.* (1996) with those of Mancktelow (1999). This issue has been explored in Zhang *et al.* (2000).

We discuss these problems in subsequent sections but foreshadow the solution here.

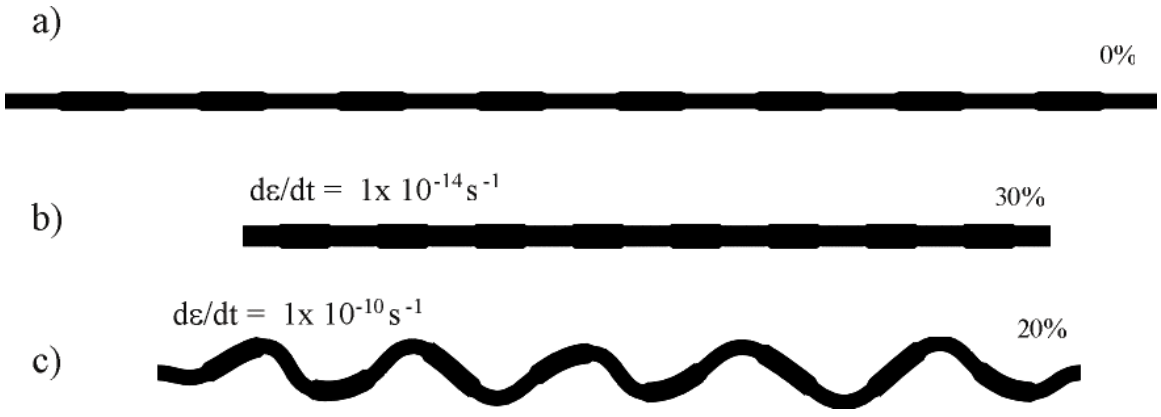

Figure 6: Folding of a layer, with initial rectangular geometrical perturbations, at two different strain rates. a) Initial geometry of the layer. b) Final layer geometry of the model with a strain rate ($d\varepsilon/dt$) of $1x10^{-14}$ s^{-1} at 30% bulk shortening; domination of homogeneous straining plus some passive amplification of initial perturbations. c) Final layer geometry of the model with a strain rate ($d\varepsilon/dt$) of $1x10^{-10}$ s^{-1} at 20% bulk shortening; domination of dynamic folding. The competency contrast (R) is 50 in both models. Corresponding material properties are: $\eta_L = 5x10^{20}$ Pa s, $\eta_e = 1x10^{19}$ Pa s, $E_L = 1.75x10^{11}$ Pa, $E_e = 3.5x10^9$ Pa, $\mu_L = 7x10^{10}$ Pa and $\mu_e = 1.4x10^9$ Pa.

In the classical Biot/Ramberg types of analyses the growth of a fold arising from a buckling instability follows a law of the type

$$w = w_o \exp(\omega t) \qquad (3)$$

where w is the displacement of the layer, w_o is a constant, ω is the growth coefficient and t is time. In general, ω is a function of stress in the layer and of competency and of competency contrasts; see for example, expression (2).

For materials which display viscosity there is also a viscous relaxation of stress once a given strain is attained.

Both the processes of viscous amplification and of viscous relaxation can be characterised by time constants which are (i) the time, ω^{-1}, for the amplitude to grow to e times the current value (where e is the base of the natural logarithms), in the case of fold amplification by buckling, or (ii) the time for the stress to decay to $1/e$ of its current value in the case of viscous relaxation.

Clearly, if the time constant for buckling amplification exceeds that for viscous relaxation, the buckling instability will grow by dynamic amplification. On the other hand, if the time constant for buckling amplification is much less than that for viscous relaxation then dynamic buckling will be very weak and the result is the domination of homogeneous deformation. We show in Section 4 that the former corresponds to the results of Zhang *et al*. (1996) whilst the latter corresponds to the results of some of Mancktelow's models (1999).

2. RHEOLOGY

In this section we briefly define terms such as *elasticity, viscosity* and *plasticity* so that our use of these terms later in the discussion is clear.

All rocks show an elastic response to an imposed stress or strain rate. This means that there is a reversible, instantaneous deformation once the stress or strain rate is applied. Commonly the stress-strain relationship is linear although non-linear response is observed at low confining pressures and strains. Non-linear elastic constitutive relationships have been appealed to recently in some folding studies (see Hunt *et al.*, 1996a,b), the response being the development of localised fold packets rather than a sinusoidal waveform with the Biot wavelength. We explore these effects further in Section 5.

It is common in geological arguments to specifically neglect elasticity under the pretext that the folding process is slow and is therefore intrinsically controlled by viscous behaviour, the elastic deformation being small compared to the viscous part of the total deformation. This is true so long as the deformation remains homogeneous throughout with no development of instabilities such as folds or shear bands.

A useful concept here is that of the Deborah Number, D_e. This is defined as

$$D_e = \frac{\text{time scale for the process of interest}}{\text{relaxation time scale}} \qquad (4)$$

Thus, for instance, if the process of interest is folding of an elastoviscous layer embedded in an elastoviscous material, the time scale for this process is the inverse of the amplification coefficient, ω, in expression (3). The relaxation time for Maxwell viscoelastic response is η/μ where η is the viscosity and μ is the elastic shear modulus (see Jaeger, 1969, p. 102).

The common geological argument that elasticity can be neglected is an assertion that the Deborah Number is less than one. This is equivalent to saying that the relaxation time scales are always large in comparison to the time scales for the growth of instabilities in the deformation with the resulting corollary that geological deformations must always be homogeneous; this quite clearly is not true.

Instabilities such as folds and shear zones grow and evolve at their own separate time scales and the mere fact that they are ubiquitous in deformed rocks means that the time scales for the growth of these instabilities exceed the relaxation time scales for the material; that is D_e is greater than one for many geological processes. Neglect of instantaneous aspects of material behaviour such as elasticity and most types of plasticity, where the constitutive behaviour is rate insensitive, is admissible only if $D_e << 1$.

As indicated above, elastic behaviour is reversible; on the other hand there are essentially two types of constitutive behaviour that describe irreversible, permanent deformational response to imposed stress or strain rate boundary conditions.

One of these modes of behaviour is typically rate insensitive but commonly strongly pressure sensitive. The rate insensitivity implies that the physical and chemical processes operating during deformation are not influenced strongly by changes in temperature whilst the strong pressure sensitivity implies that these processes have a strong normal stress dependence, that is, they have a frictional character. Thus, the commonly accepted mechanism of deformation for these materials is fracturing and sliding on these fractures. Such processes can operate at all scales from the micro- or grain-scale, where the structures involved are microcracks or grain boundaries, to the regional scale where the structures involved are joints, fault systems and bedding planes.

The style of deformation described above is called *plasticity* and commonly the constitutive behaviour is described using a Mohr-Coulomb Yield Criterion with an associated or non-associated flow rule. We do not explore materials characterised by plastic behaviour in this paper. Examples of the folding of plastic materials can be found in Chapple (1969) and in Zhang *et al*. (1996). It appears that strain localisation behaviour of plastic materials strongly affects the buckling development of a plastic layer, resulting in more localised buckling growth in comparison with elastic or viscous materials.

The second of these irreversible modes of deformation is just the opposite to plasticity: the mechanical behaviour is strongly rate sensitive but pressure insensitive. This implies that the mechanisms of deformation are strongly temperature dependent but not dependent on changes in normal stress. The commonly accepted mechanisms of deformation for these materials are grain-scale crystal defect processes with or without atomic diffusion.

This style of deformation is called *viscosity* and commonly the constitutive behaviour is described in terms of a power-law dependence of the viscosity upon the strain rate. The constitutive relationship is

$$\sigma'_{ij} = 2\eta D_{ij} \tag{5}$$

where σ'_{ij} are the components of the deviatoric stress tensor, D_{ij} are the components of the stretching and η is the viscosity, given by

$$\eta = \eta_0 (\dot{\gamma}/\dot{\gamma}_0)^{N-1} \tag{6}$$

where η_0 and $\dot{\gamma}_0$ are the reference viscosity and strain rate, and $\dot{\gamma}$ is the equivalent strain rate. N is a constant which for many geological materials has values in the range 0.3 to 1. If N=1 the constitutive behaviour is called *Newtonian Viscosity*. The constitutive behaviour described by (5) is a coaxial constitutive law in that the principal axes of stress are always coaxial with the principal axes of the deformation rate.

Almost all of the literature on folding is concerned with linearly elastic materials, or Newtonian viscous materials or combinations of one of these materials embedded in the other. The results of studies of these materials predicts the operation of a Biot type wavelength selection process with the ultimate exponential amplification of a single dominant wavelength independent

of the geometry of initial irregularities in the layer. Thus the resultant geometry is always periodic with one wavelength.

A much more interesting constitutive behaviour is the simple Maxwell elastoviscous material (see Jaeger, 1969, p. 102). This consists of a linear elastic element in series with a Newtonian viscous element. We are just starting to understand the complexity in behaviour that such Maxwell materials can exhibit during single layer folding. We explore some of this complexity in Section 4.

3. FOLD GROWTH IN PURELY ELASTIC OR PURELY VISCOUS MATERIALS

There is a large literature on the buckling of single layer linearly elastic materials embedded in both linearly elastic and viscous materials. Since no interesting geological materials are likely to be purely elastic in the deformation ranges associated with folding, we do not consider these materials any further here; good treatments of such materials can be found in Biot (1965) and Mühlhaus (1993).

Again, the literature on buckling of single layer, viscous materials embedded in like materials is very large. All of the analyses except those of Ghosh (1970), Fletcher (1991) and of Mühlhaus *et al*. (1998) are for two dimensional situations and except for Fletcher (1974), Smith (1977 and 1979), Lan and Hudleston (1991), Abbassi and Mancktelow (1992), Mancktelow and Abbassi, (1992), Hudleston and Lan (1994), parts of Johnson and Fletcher (1994), Mühlhaus *et al*. (1998) and Mancktelow (1999) the constitutive relationship is Newtonian viscous; the latter papers involve power law viscous materials. A detailed discussion of the buckling behaviour of Newtonian viscous materials is given by Biot (1965), Hudleston (1973), Price and Cosgrove (1990) and Johnson and Fletcher (1994).

The important results that arise from these studies of buckling in viscous (Newtonian and non-Newtonian) materials are:

(i) For all viscous materials just one dominant wavelength develops for a two dimensional situation (see however Johnson and Fletcher, 1994, p. 379). This wavelength is given by expression (1). However, it is only for Newtonian viscous materials that the viscosity is independent of strain rate. For viscous materials where N in expression (6) is not equal to one, the viscosity is a function of strain rate as indicated by expression (6). Hence, a simple expression for the dominant wavelength for materials with N ? 1 is not available (note that expression (1) holds only for viscous materials with N=1). However Mühlhaus *et al*. (1998) plot dispersion curves (ie growth rate versus the wave number) for materials with N=1, N=0.5 (see their Figures 1, 2, 3, and 4); as is to be expected, for N=1 the dominant wavelength is always given by expression (1), however for N=0.5, with the viscosity defined by (6), the dominant wavelength is approximately 0.8 of that predicted by expression (1). The conclusion is that for viscous materials with N<1, the dominant wavelength is less than the Biot wavelength predicted by (1), using the viscosity defined by (6).

(ii) In three dimensions, both elastic and viscous materials develop two wavelengths, one "dominant" wavelength normal to the maximum shortening rate and another "subsidiary" wavelength normal to the intermediate shortening rate (see Figure 7 and Figure 8). Thus, fold patterns resembling interference structures can develop. Neither of these wavelengths coincide with the classical Biot wavelength except in special circumstances.

a)

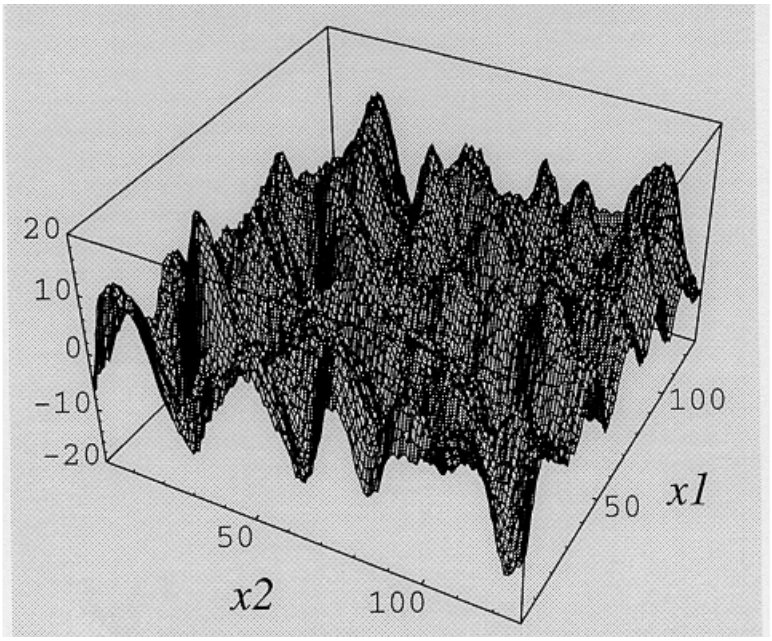

b)

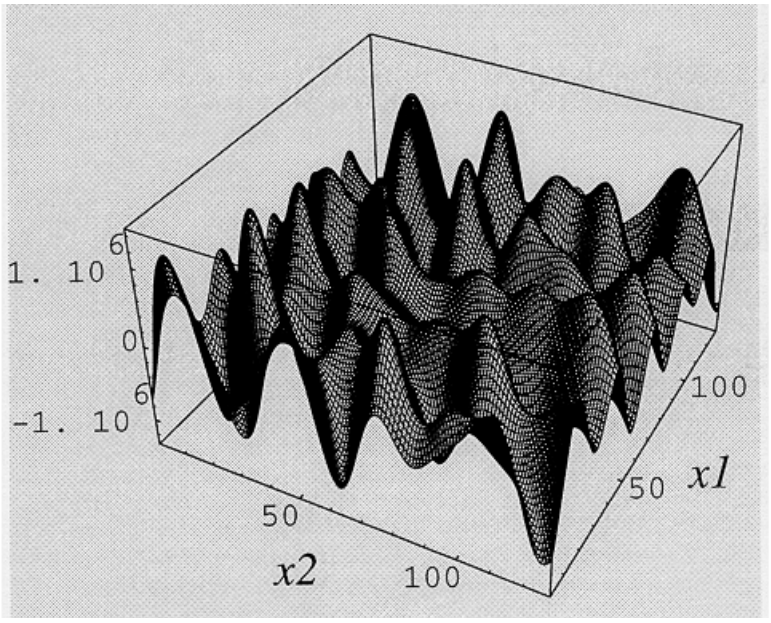

Figure 7: Fold system developed in viscous single layer with power law exponent = 0.5 (N in expression 6). Deformation rates equal parallel to x_1 and x_2. a) Shortening 15.9% for R_{visc}=60; initial perturbations still visible. b) Shortening 12% for R_{visc}=600 (After Mühlhaus *et al.*, 1998).

a)

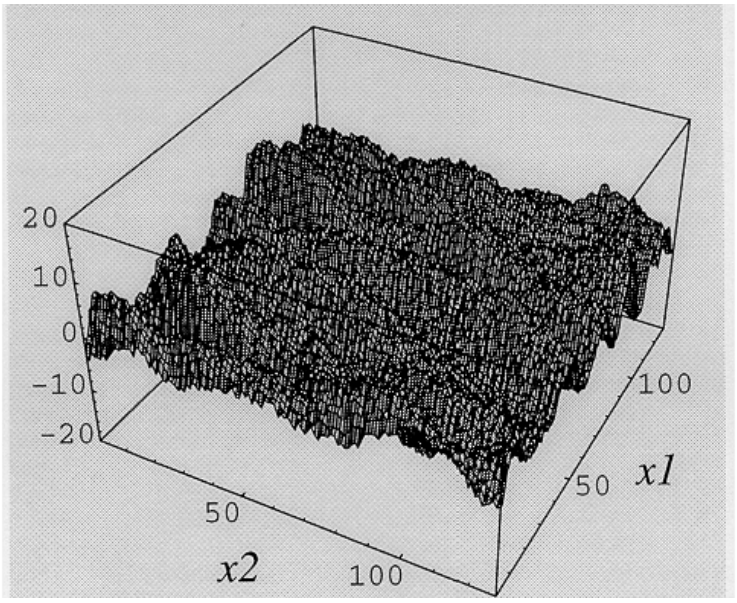

b)

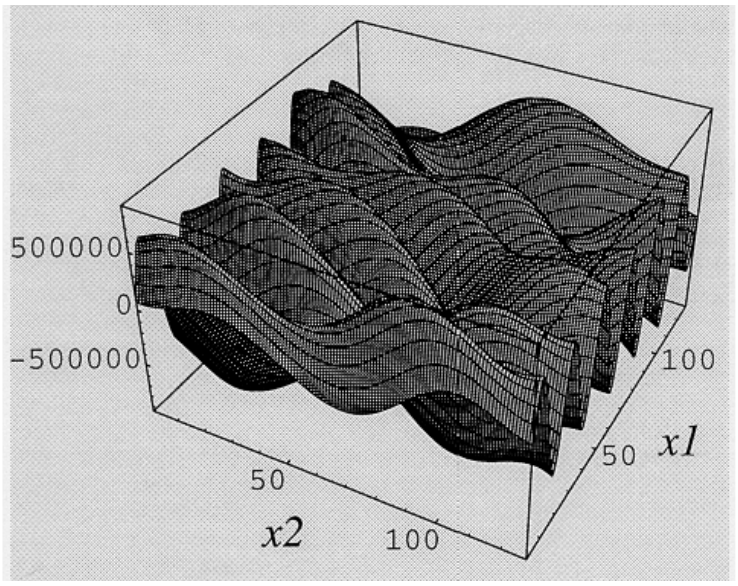

Figure 8: Fold system developed in viscous single layer with power law exponent = 0.5 (N in expression 6). Plane straining, that is, the deformation rate parallel to x_2 is zero. a) Shortening 135% for R_{visc}=60; initial perturbations still visible. b) Shortening 18% for R_{visc}=600 (After Mühlhaus *et al.*, 1998).

4. FOLD GROWTH IN ELASTOVISCOUS MATERIALS

A study of fold growth in elastoviscous materials is particularly instructive since the range of possible behaviours is exceedingly rich. In part this is because there exist three time scales: the relaxation times of the single layer material and the embedding material respectively and the time scale associated with the fold evolution. If the time scale of the fold evolution is much slower than both relaxation times then the system behaves approximately like a viscous layer embedded in a viscous matrix. If, on the other hand, the fold evolution is much faster than both relaxation times then elastic in elastic behaviour ensues and so on.

This leads to a strong dependence of folding behaviour on strain rate. In what follows we concentrate on the simple Maxwell elastoviscous material.

As indicated in Section 2 the Maxwell elastoviscous material consists of a linear elastic element in series with a viscous material (see Jaeger, 1969, p. 102). The relaxation time, ξ, for such a material is $\xi = \eta/\mu$ where η is the viscosity of the viscous element and μ is the shear modulus for the elastic element.

If ω is the amplification factor from (3), then Mühlhaus *et al*. (1998) show that it is convenient to define a dimensionless quantity, ς, as $\varsigma = \xi\omega$. Then, the behaviour of single layer Maxwell systems can be rationalised by examining various regimes for ψ where

$$\psi = 1 - \varsigma_L \varsigma_e^2 \qquad (7)$$

The function $\varsigma_L = \varsigma_e^{-2}$ is plotted in Figure 9.

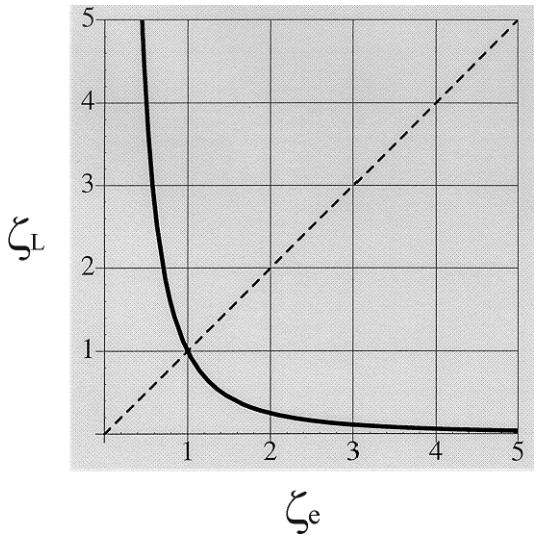

Figure 9: Domains of qualitatively different behaviour in dependency of the relaxation times ς_L of the plate material and ς_e of the supporting material. Spontaneous buckling instability occurs if $\varsigma_L > (1/\varsigma_e)^2$ leading to the generation of two "dominant" wavelengths. $\varsigma_L = (1/\varsigma_e)^2$ is shown as a solid line; $\varsigma_L = \varsigma_e$ is shown as a dashed line.

If $\psi \geq 0$ only one dominant wavelength develops. Examples of the dispersion function are given in Figure 10(a) and Figure 10(b). However, if $\psi < 0$ two dominant wavelengths develop; the dispersion function is shown for $\varsigma_L = 4$, $\varsigma_e = 1.5$ in Figure 10(c). These results are based on a linear stability analysis and some results of the growth of buckling instabilities within the various regimes of Figure 9 are given in Figure 11.

It is the development of two dominant wavelengths for the buckling of Maxwell materials that is perhaps the origin of parasitic folds in natural fold systems. Such behaviour is not possible in linear elastic or Newtonian viscous materials although such behaviour is perhaps possible in other non linear rheologies which have not yet been explored. Notice however that fold systems such as those shown in Figure 11 are still quite regular in that they result from the superposition of two periodic wavetrains of two different wavelengths. There is still none of the irregularity demonstrated by natural folds (see Figure 2 and Figure 3).

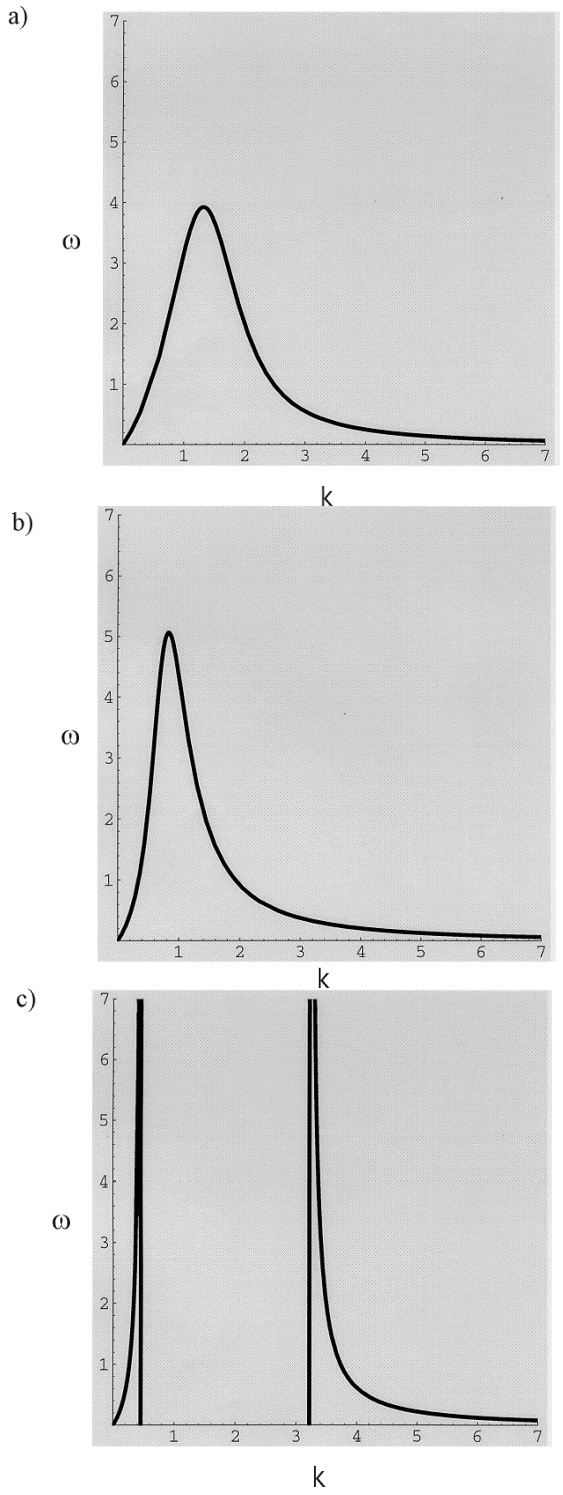

Figure 10: a) Dispersion function for D_2=0, N=1.0, $\psi = 1 - \varsigma_L \varsigma_e^2 > 0 : \varsigma_L = 1.5$ and $\varsigma_e = 0.5$. b) Dispersion function for D_2=0, N=1.0, $\psi = 1 - \varsigma_L \varsigma_e^2 > 0 : \varsigma_L = 0.5$ and $\varsigma_e = 1.0$. c) Dispersion function for relaxation time in the region for $\psi = 1 - \varsigma_L \varsigma_e^2 < 0 : \varsigma_L = 4.0$ and $\varsigma_e = 1.5$. Notice two wavenumbers are now amplified. The value of 1.0 for the wavenumber corresponds to the Biot wavelength given by expression (1).

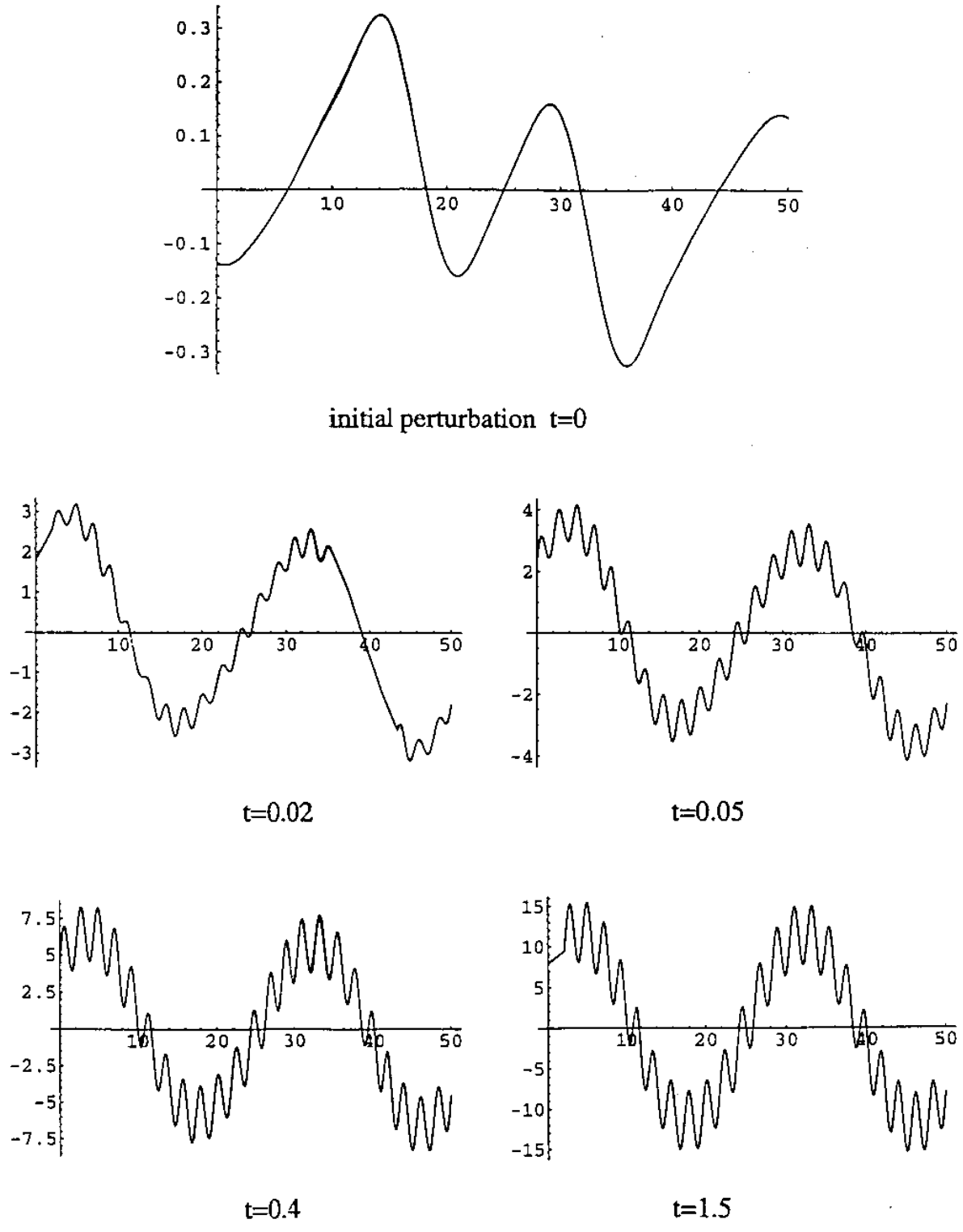

Figure 11: Numerical solutions for growth of fold system in the field $\psi < 0$ in Figure 9; $\varsigma_L = 3$ and $\varsigma_e = 3$. The indicated times are dimensionless and are fractions of the viscous, fold amplification, time constant.

However there is another extremely important aspect of the buckling of Maxwell materials; namely a strong dependence of fold amplification upon strain rate, viscosity, elastic moduli and competency contrast. Under some combinations of these four variables, the model shown in Figure 1 undergoes only homogeneous shortening with no wavelength selection processes operating and, hence, no buckling processes. This is the type of behaviour illustrated in Figure 6(b). Under other combinations, buckling is well developed as in the case of Figure 6(c). As has been alluded to earlier in this paper, whether the homogeneous shortening mode or the pure buckling mode dominates in a particular situation depends on the competition between the viscous relaxation rate and the buckling amplification rate and is expressed through the Deborah Number given in (4). The situation is treated and illustrated in the sequence of papers: Zhang *et al*. (1996), Mancktelow (1999), Zhang *et al*. (1999 a,b,c), and Zhang *et al*. (2000).

One important aspect of this behaviour is that initial geometrical perturbations are preserved and amplified in an entirely passive manner or a manner characterized by initial passive amplification (limb dips reach higher angles) plus later dynamic growth at one end of the spectrum of behaviour, where homogeneous shortening plays a critical role. Such initial geometrical perturbations tend to be obliterated at the other end of the spectrum of behaviour where wavelength selection processes operate and one or more wavelengths become dynamically amplified. For buckling at this end of the spectrum, the mechanical ability of the system to be able to select new wavelengths related to competency contrast and layer thickness is critical. This means that with such an ability, a weak layer (small competency contrast) would not support the growth of initial broad geometrical perturbations (initial wavelength too large), and similarly a strong layer (large competency contrast) would not support the growth of initial very small perturbations (initial wavelengths too small). These aspects are illustrated in Figure 6 but also in Figure 12 to Figure 14.

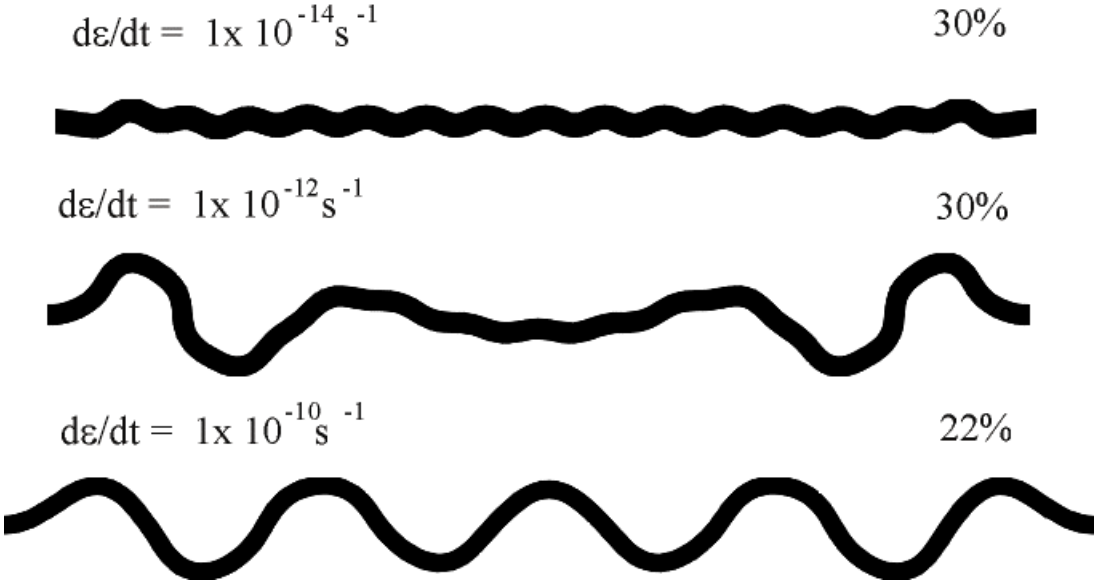

Figure 12: Enhancement of dynamic fold growth by increasing strain rate (dε/dt). Competency contrast (R) is 200 in all three models. Corresponding material properties are: $\eta_L = 2x10^{21}$ Pa s, $\eta_e = 1x10^{19}$ Pa s, $E_L = 7x10^{11}$ Pa, $E_e = 3.5x10^9$ Pa, $\mu_L = 2.8x10^{11}$ Pa and $\mu_e = 1.4x10^9$ Pa. Note that in the model with $d\varepsilon/dt = 1x\ 10^{-14}\ s^{-1}$, the dynamic fold growth rate is very small so that homogeneous straining is dominating at the 30% bulk shortening stage.

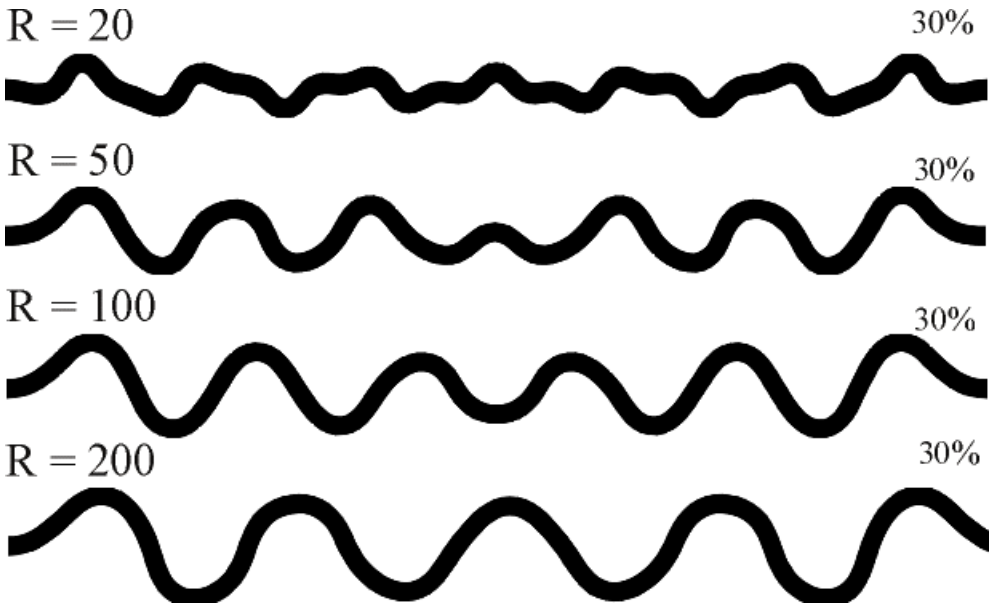

Figure 13: Enhancement of dynamic fold growth with increasing competency contrast (R) between the layer and the medium at a particular strain rate ($d\varepsilon/dt = 1x10^{-14}\ s^{-1}$ for all the models). Material properties for the model with R = 20 are: $\eta_L = 2x10^{23}$ Pa s, $\eta_e = 1x10^{22}$ Pa s, $E_L = 3.5x10^{10}$ Pa, $E_e = 1.75x10^9$ Pa, $\mu_L = 1.4x10^{10}$ Pa and $\mu_e = 0.7x10^9$ Pa. For the other models parameters for the medium (η_e, E_e and μ_e) are decreased to form the indicated R values.

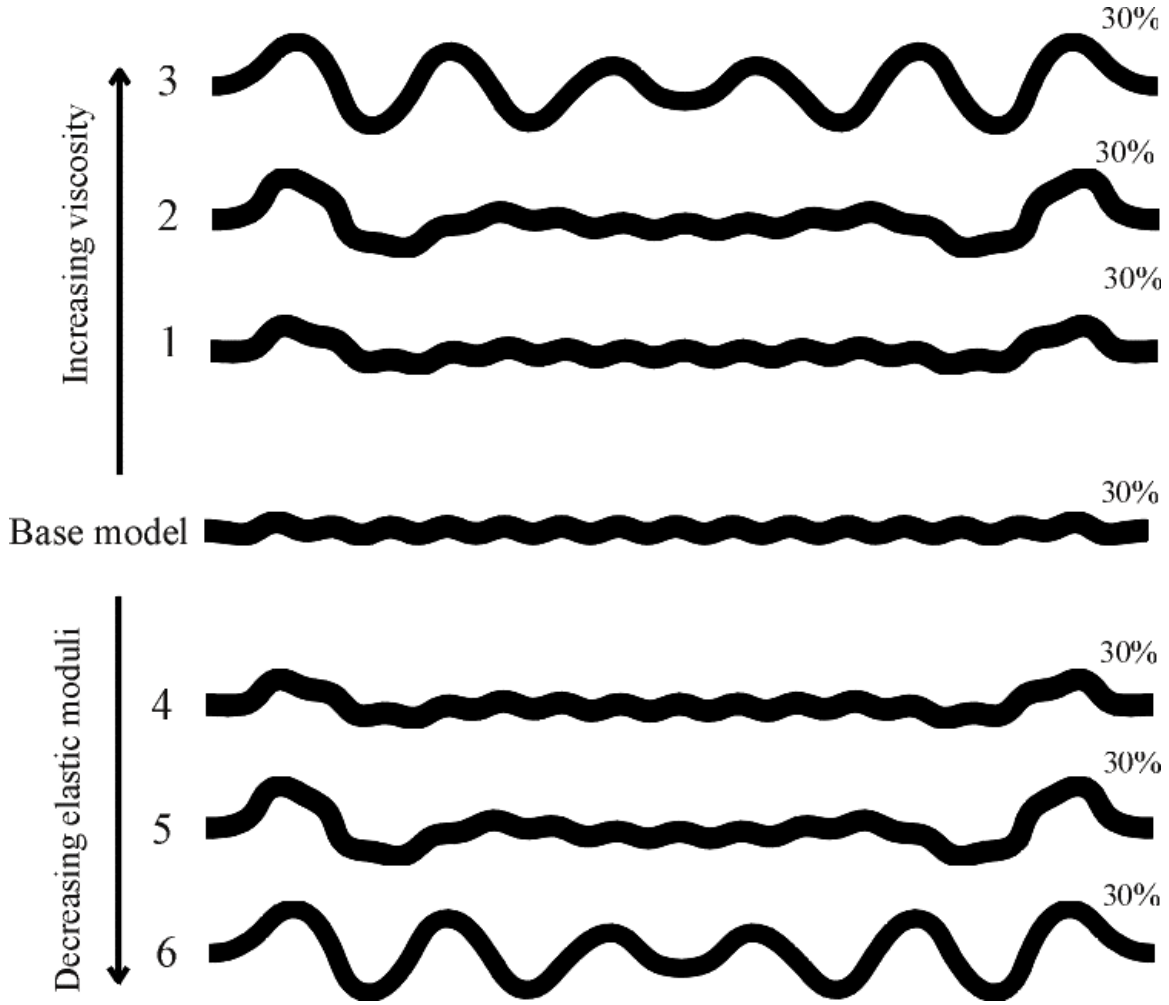

Figure 14: Enhancement of dynamic fold growth with increasing viscosity or with decreasing elastic moduli at a particular strain rate and competency contrast ($d\varepsilon/dt = 1x10^{-14}$ s^{-1} and R = 100 for all the models). Material properties for base model are: $\eta_L = 1x10^{21}$ Pa s, $\eta_e = 1x10^{19}$ Pa s, $E_L = 3.5x10^{11}$ Pa, $E_e = 3.5x10^{9}$ Pa, $\mu_L = 1.4x10^{11}$ Pa and $\mu_e = 1.4x10^{9}$ Pa. Viscosity (η_L and η_e) are increased by 10, 100 and 1000 times in model 1, 2 and 3, with respect to the base model. Elastic moduli (E_L, E_e, μ_L and μ_e) are decreased by 10, 100 and 1000 times in model 4, 5 and 6, with respect to the base model. Note that the base model is dominated by homogeneous shortening and passive amplification of initial geometrical perturbations, similar to the results of one of Macktelow's (1999) finite element models.

The essential processes operating here are:

(i) Increasing strain rate has the effect of decreasing the importance of homogeneous straining and enhancing dynamic amplification. This is demonstrated in Figure 12 which shows the results of a series of numerical experiments at 10^{-14} s^{-1}, 10^{-12} s^{-1} and 10^{-10} s^{-1} strain rate. For the identical initial geometry and material properties, buckling behaviour varies from the domination of homogeneous shortening and passive amplification of initial geometrical perturbations at a strain rate of 10^{-14} s^{-1} (this is similar to the results of Mancktelow, 1999) to the domination of dynamic folding at 10^{-10} s^{-1}.

(ii) Increasing the competency contrast (R) at a particular strain rate increases the tendency towards dynamic fold amplification as shown in Figure 13. Note that the model with a small competency contrast (R=20) displays a more irregular fold train due to relatively weak dynamic fold growth and this seems to be closer to fold geometries observed in Nature.

(iii) Decreasing the absolute value of the elastic moduli for the folding layer increases the tendency towards dynamic amplification as shown Figure 14 (bottom part).

(iv) Increasing the absolute value of the viscosity for the folding layer increases the tendency towards dynamic amplification as shown Figure 14 (top part). This can have an identical effect on folding as decreasing the value of the elastic moduli.

5. FOLD GROWTH IN MORE EXOTIC MATERIALS

The previous section showed the increase in complexity that can arise in coupling elasticity with viscosity in a simple Maxwell material. Although there has only been a limited amount of work done on more complicated materials, the characteristics of materials with coupled elastic and viscous constitutive behaviour seem to be fundamental in allowing single layers to deform into fold systems that are irregular or even chaotic with respect to the spatial distribution of wavelengths. For some such materials localisation of buckles develop; these can combine to produce irregular fold systems. In other materials the folding processes is deterministically chaotic so that the final buckled configuration is inherently sensitive to initial conditions.

In this context we emphasize that the results of the previous section, demonstrating the development of two dominant wavelengths in a buckling Maxwell layer, are based on a linear stability analysis. If one were prone to speculation, one could perhaps contemplate that a full non-linear analysis would demonstrate that such a result is part of a period doubling sequence on the route to chaos (see for instance Holmes, 1990) even for a simple Maxwell material. We await such a non-linear stability analysis with considerable interest.

We explore some non-linear behaviour briefly below.

In searching for the origin of irregular behaviour during buckling, the role of geometric and/or physical non-linearities on the folding process has been investigated many times. Yield points or high power law exponents cause sharper fold crests; more accurate geometric modelling introduces cubic non-linearities increasing the vigour of the instability. Both refinements lead to quantitative changes; they however do not introduce qualitative changes, or more or higher complexity in the model. As mentioned above, one way of introducing complexity is by considering the competition of multiple time scales; another way is to consider non-linearities related to kinematic control of the fold amplitude through prescribed axial velocities at the fold edges (see Budd *et al*., 1998; Budd and Peletier, 1998). It can be shown that these constraints:

- exclude periodicity of the fold amplitude distribution at all times
- increase the fold amplitude according to a power law with a power law exponent of 1/8 and not exponentially as predicted by the linear theory and expressed in (3), and
- decrease simultaneously the axial load, and the driving force of the instability with the square root of the time.

The analysis of non-linear systems with respect to buckling single layers is divided into two categories. The first category involves the analysis of non-linear constitutive laws such as Kelvin-Voigt materials (linear spring plus viscous element in parallel) and combinations of Maxwell and Kelvin-Voigt materials (Hunt *et al*., 1997), softening elastic layers embedded in Maxwell materials (Hunt *et al*., 1996a), an elastic layer in a softening Maxwell material (Hunt *et al*., 1996b; Whiting and Hunt, 1997) and simple non-linear mechanical systems comprised of rigid rods linked by elastic springs (Hunt and Lawther, 1999).

These analyses lead to a number of different types of solutions for the waveforms that grow. Some are illustrated in Figure 15. A feature of many such analyses is the formation of

localized packets of folds (Figure 15(c), (d)) rather than an extended periodic waveform (Figure 6(c)) that is characteristic of the classical Biot-type results.

Another aspect of these non-linear approaches is the development of chaotic features of the folding process. By "chaotic" here we mean to imply a strong dependence of the fold geometry upon initial conditions and the formation of non-periodic solutions. As an example we reproduce some of the results from Hunt *et al*. (1996a).

The model comprises an elastic layer supported by a special Maxwell material which provides elastoviscous resistance against vertical, but not horizontal, movement (Figure 16). Notice here that the vertical deflection of the layer is *w* (x) where x is the spatial dimension measured along the layer. The elastic moduli of the Maxwell material are allowed to soften as the deformation proceeds. This non-linearity allows localisations, or packages of folds, to develop in the layer as shown in Figure 15. The chaotic and fractal nature of this kind of folding process is illustrated by Figure 17. We ask: What happens to an initial condition of deformation for the layer specified by a point in the four-dimensional space $(w, w', w''w''')$ where a prime denotes differentiation with respect to x? Does such an initial deformation lead to a localisation or not? And how far along the layer, measured by x in Figure 16, does the localisation occur? On a plane normal to x and distant x_{div} from the origin we then plot a white dot if no localisation occurs at x_{div} or a black dot if localisation does occur (see Figure 17).

We see that as we move progressively along the layer the plot of localisation versus no-localisation adopts a fractal character. Figure 15 is in fact a plot of the various localisations that occur within the small circled area on Figure 17 for $x_{div} = 180$. Each one of these localisations corresponds to one of the black dots within the circle and each is separated from the next by a white region in this figure. In fact, the regions shown by $x_{div} = 100$ and $x_{div} = 180$ are completely fractal and may be magnified indefinitely to still give a black and white banded structure (see Hunt *et al*., 1993 for such magnification).

This example shows a characteristic that is common to most of the approaches to buckling that involve strong non-linear constitutive relations, namely that the final buckled configuration is extremely sensitive to initial conditions since initial configurations very close to each other in (w, w', w'', w''') space can lead to either no localisation or completely different patterns of localisation. This extreme sensitivity to initial conditions is the hallmark of a chaotic system.

The second category involving the analysis of non-linear systems within the context of buckling of single layers involves the incorporation of microstructural evolution into the constitutive behaviour and feedback relations involving the influence of flow stress upon the microstructure.

This approach promises to provide a unifying theory of geological deformation whereby microstructural and microfabric evolution can be linked to macro-scale deformation features such as fold systems.

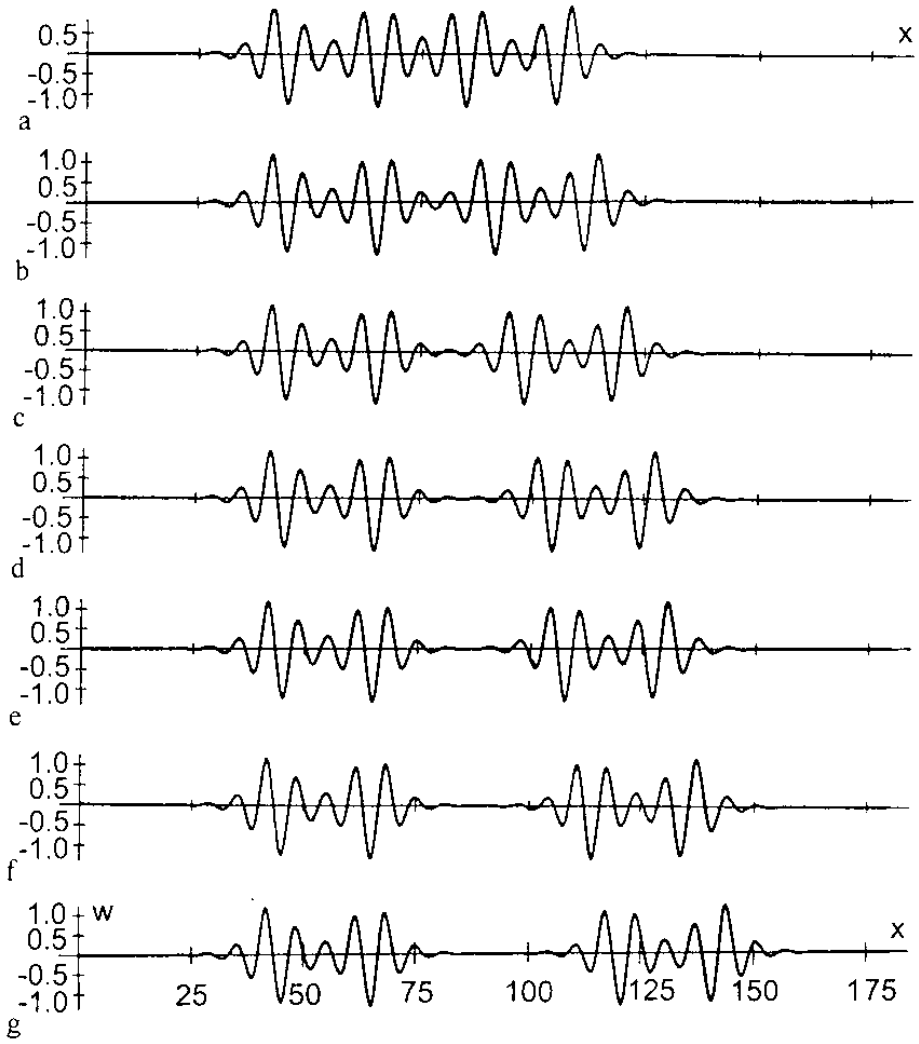

Figure 15: Localised fold packets developed in a single layer elastoviscous material with elastic shortening. *x* **is the distance measured along the layer as shown in Figure 16.** *w* **is the deflection of the layer shown in Figure 16. Each localised fold system corresponds to slightly different initial conditions.**

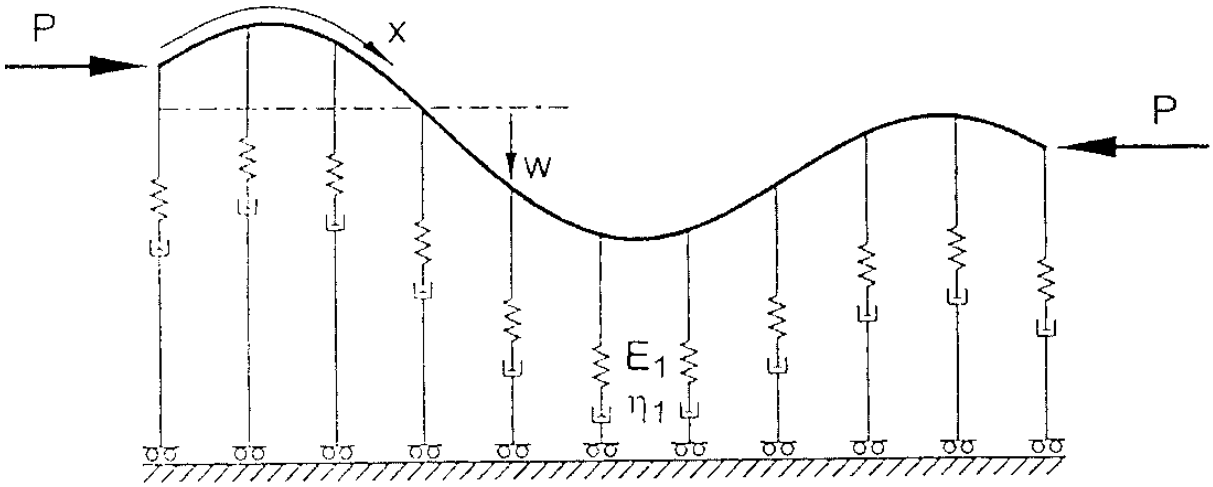

Figure 16: Geometry of the model which produces the localised fold packets of Figure 15. The elastic layer is compressed by a force P and is embedded in a viscoelastic material of Youngs Modulus E_1 and viscosity η_1.

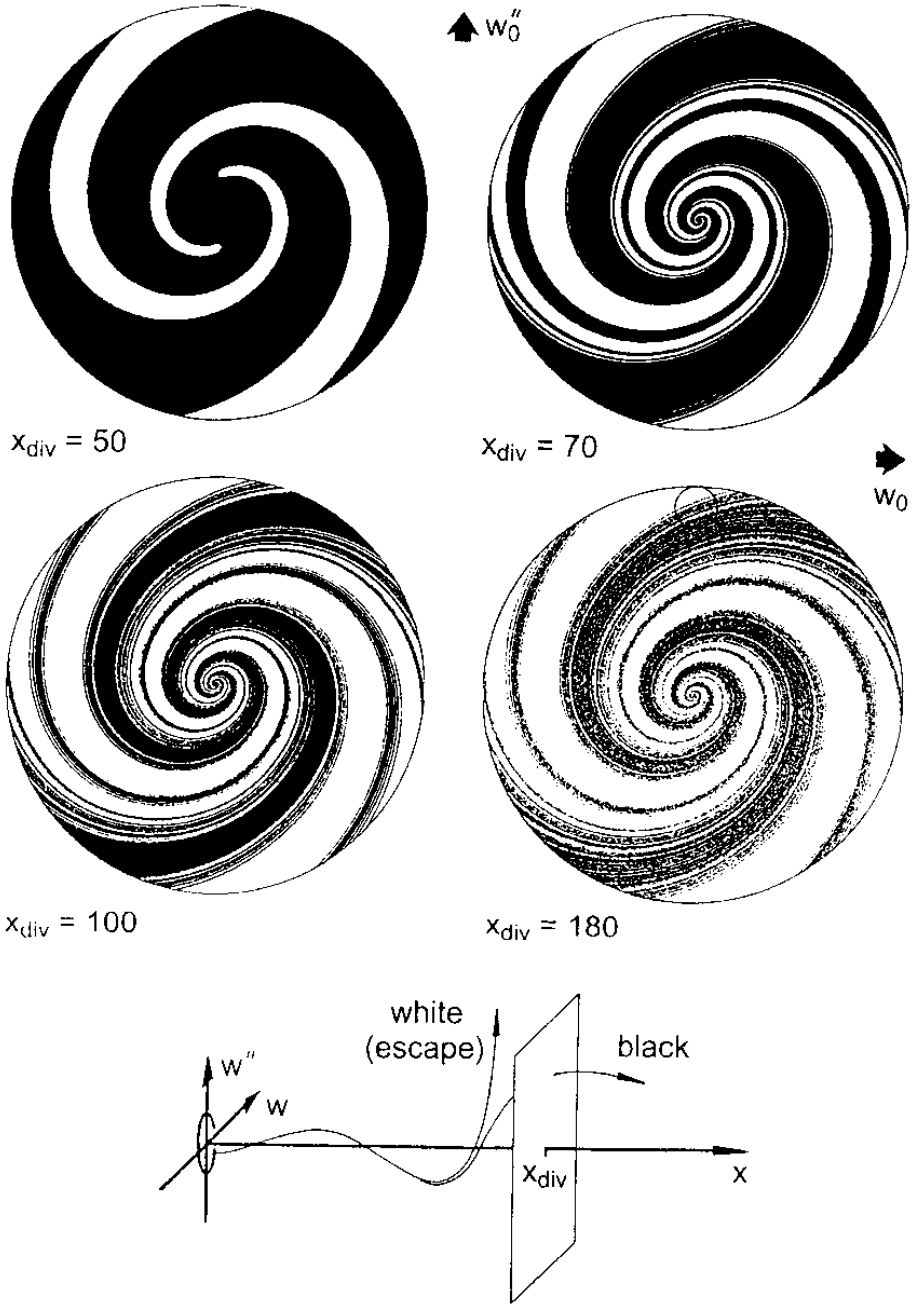

Figure 17: Plots of initial conditions (defined in this diagram by various positions in (*w*,*w'*) space) which either do (white) or do not (black) lead to the development of a localised fold package at distance x_{div} along the layer. The various plots in Figure 15 are derived from the initial conditions represented in the small circle shown on the plot for $x_{div} = 180$.

All previous work on the mechanics of folding has been at what one might call a macro-level: the buckling layer and its embedding medium are considered, in turn, to be homogeneous and isotropic with respect to their constitutive parameters and the role of microstructure is

completely neglected. Yet it is clear that as rocks undergo the folding process, evolution of microstructure is intimately associated with the changing deformation history in various parts of the fold. Even more, the deformational history at each point in a deforming layer influences the patterns of crystallographic preferred orientation in concert with changes in grain shape, grain size distribution and the degree of recrystallisation. Each one of these textural and microstructural attributes is not only influenced by the deformation history but itself directly influences the flow stress. Thus, there is a feedback loop of the type.

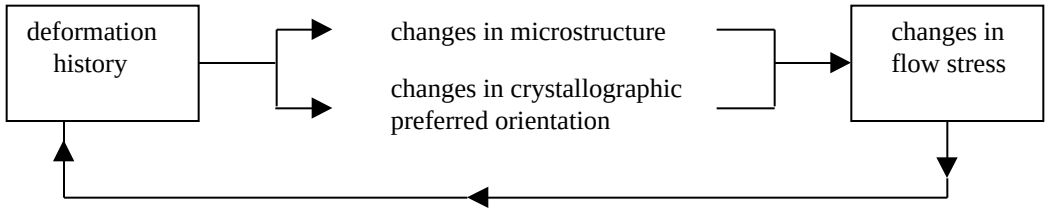

Hence, for instance, since the deformation history at a fold hinge (consisting of pure coaxial shortening) is quite different to that on a fold limb (consisting of, initially, pure coaxial shortening followed later by non-coaxial shearing) we expect the microstructure and the crystallographic preferred orientations to be different in these two deformation regimes. Such differences have been well documented over the past seventy years (see for instance Sander, 1930). The important point here is that such microstructural and crystallographic preferred orientation differences imply different flow stress in different parts of the fold.

We explore this relationship between folding and microfabric development in a little more detail below with emphasis on grain size development during folding.

Grain size evolution relationships have been considered by authors such as Derby and Ashby (1987), Kameyama et al. (1997), and Karato et al. (1986). An interesting discussion of the phenomenology of domain boundary migration can be found on the www version of a poster by Bons *et al.* (1997). Recently, Braun et al. (1999) proposed an evolution relationship of the form

$$\dot{d} = -\frac{\dot{\gamma}}{\gamma_T}\left(d - d_\infty\right) \qquad (8)$$

where d is the grain size, $\dot{\gamma}$ is the deformation rate, γ_T is the characteristic strain required to reach a steady state grain size, d_∞. This evolution law was introduced in the context of the transition (and competition) between dislocation creep and grain-size sensitive creep. The steady state grain size, d_∞, is given by

$$d_\infty = B d_0 \left(\frac{\tau}{\tau_0}\right)^{-p}, \qquad (9)$$

where d_0 and τ_0 are a reference grain size and reference stress respectively. How do grain sizes evolve in response to the highly non-linear loading history during folding? The scenarios we have in mind involve rather extreme deformations. We consider isothermal viscous flow.

For the viscosity we assume a power law dependence on grain size (Karato and Wu, 1993).

$$\eta = \eta_0 \left(\frac{d}{d_0} \right)^m . \qquad (10)$$

Our model folding scenario consists of five initially parallel layers of different viscosity (Figure 18). The initial geometry and the material properties are symmetric with respect to the horizontal centre line. The viscosity of the centre layer is largest and that of the outer layers is smaller. The outermost layer is present only as a computational necessity, so it is assumed to be highly compressible so that it provides virtually no impediment to folding. In all calculations we assume that $\eta_0^{(1)}/\eta_0^{(2)}/\eta_0^{(3)} = 8\,0\,0 / 1$ and that $m^{(1)}=m^{(3)}=0$. At the beginning of the calculations (t=0), we assume that $d=d_0$ everywhere. The layered block is strained by assuming a constant horizontal velocity, $v_0 = -5$, at the right boundary. All other boundaries have no normal velocity and zero tangential stresses – this is equivalent to a symmetry plane. A small perturbation in the thickness of the middle layer is used to provide a trigger of the folding instability.

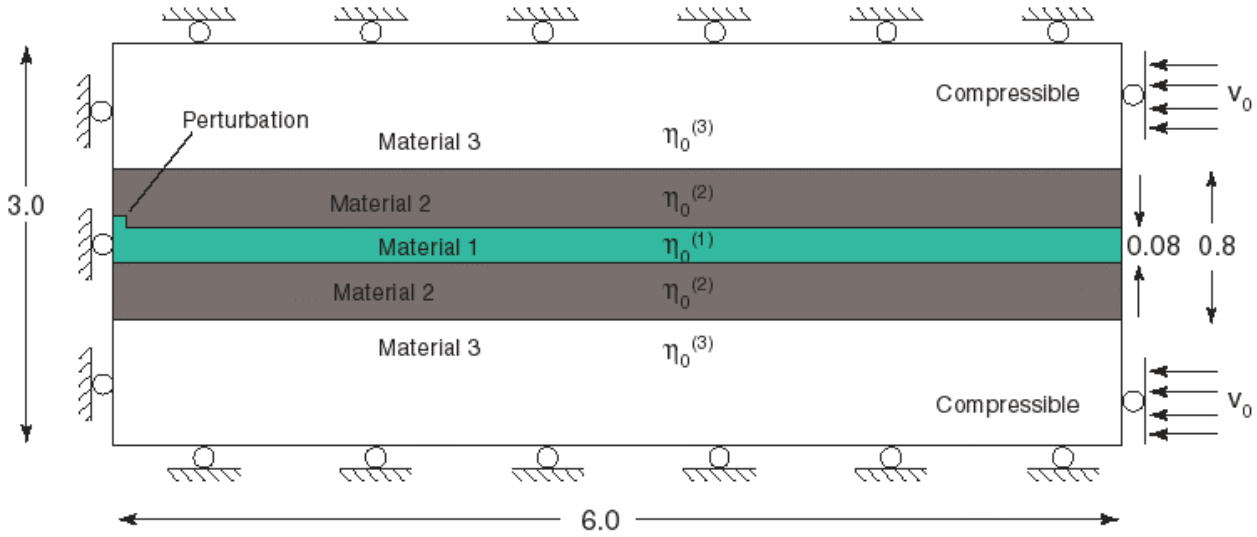

FIGURE 18. The initial state of the simulation showing boundary conditions on the solution domain.

As mentioned earlier, we are interested in large deformations which are sufficiently large that they would usually be associated with severe numerical difficulties when using updated or total Lagrangian schemes. At the heart of the problem is the ill-conditioning of the stiffness matrices due to mesh entanglement or close-to-singular Jacobians. Here we circumvent these problems by applying a finite element based material point method (Moresi *et al.*, 2000, Mühlhaus *et al.*, 2000)

The method uses a fixed usually regular grid and integrates the stiffness matrices and force vectors based on the information momentarily carried by a finite number of material points, ideally between 4-10 per finite element. After each time step the position of the material points (relative to a spatially fixed mesh) is updated (points may cross element boundaries) and the computational cycle continues.

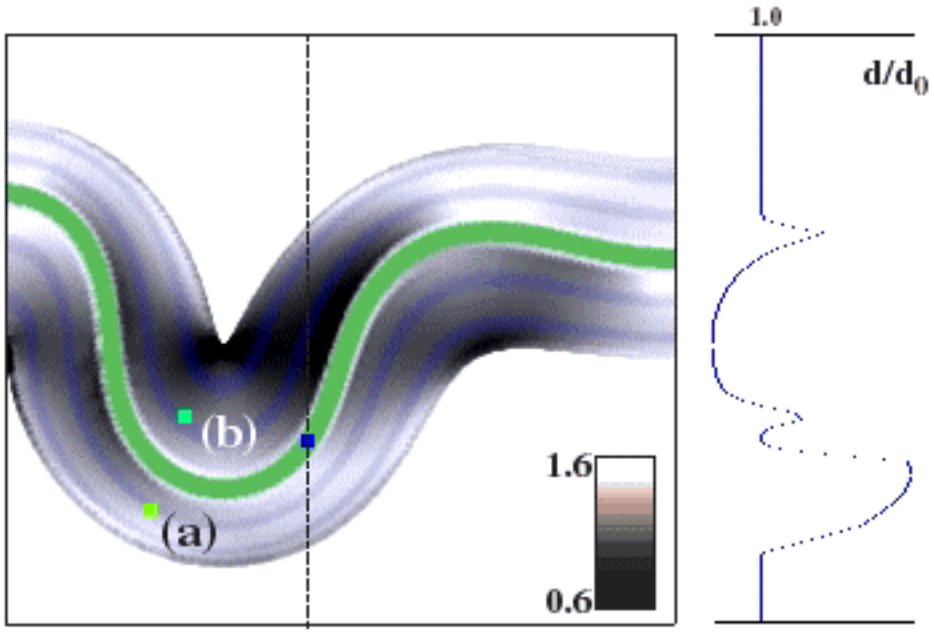

FIGURE 19. After 44% axial shortening, the material has folded and grain sizes have evolved as shown in the shading. A profile of grain size along the dashed line is shown on the right. Points (a,b) were originally located in the same vertical plane. They are fixed within the material and serve to record grain growth for a specific place during the simulation.

Figure 19 shows the deformation at 44% axial shortening of the block. The shading in the figure indicates the prevailing grain size, with dark shading indicating regions where the grains are smallest. In this example, $m^{(2)}=0$, so grain size evolution does not affect the deformation. However, the deformation affects the grain growth through τ in (9) and $\dot{\gamma} = \sqrt{2D_{ij}D_{ij}}$ in (8).

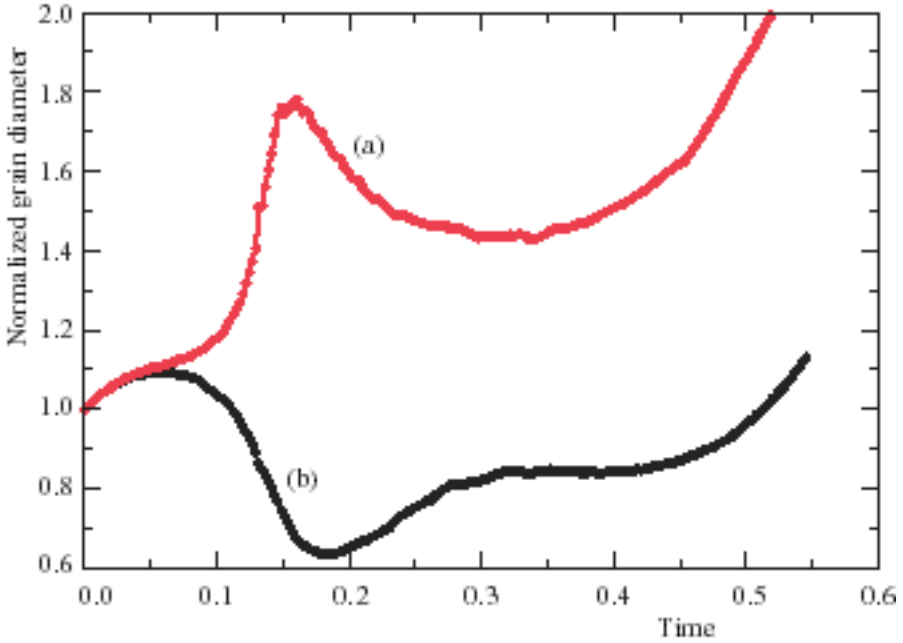

Figure 20: Normalized grain diameter for the points (a,b) shown in Figure 19 as a function of time during the simulation.

In Figure 20 we have plotted the history of the grain sizes at locations (a,b) in Figure 19. There is an initial adjustment phase in which grains everywhere grow uniformly due to the supplied compressive load. However, as the fold grows, the loading of different points such as (a) and (b) diverges. (a) is unloaded through time and shows pronounced grain growth. (b) is initially loaded and the grains become smaller but, at a later time, the stress is concentrated around the region of highest curvature away from (b).

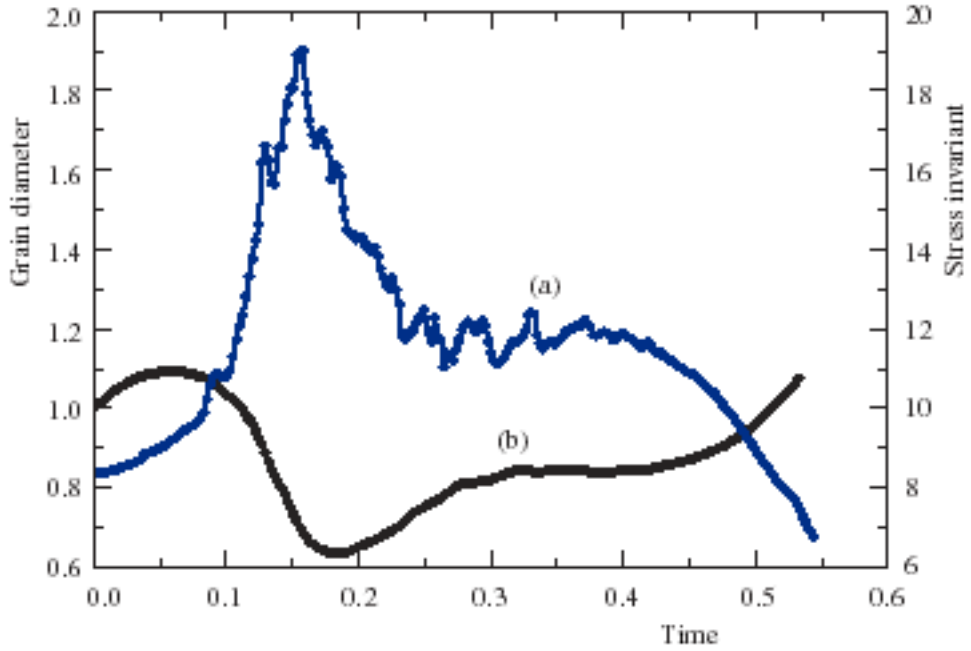

Figure 21: Deviatoric stress invariant (a), and normalized grain diameter (b) for the point (b) shown in Figure 19 as a function of time during the simulation.

In Figure 21 we plot the stress history for point (b) along with the grainsize variation. There is a clear correlation between the deviatoric stress invariants and the corresponding grain sizes indicating that, with the parameters we have chosen, the timescale of grain evolution is essentially enslaved by the structural timescale.

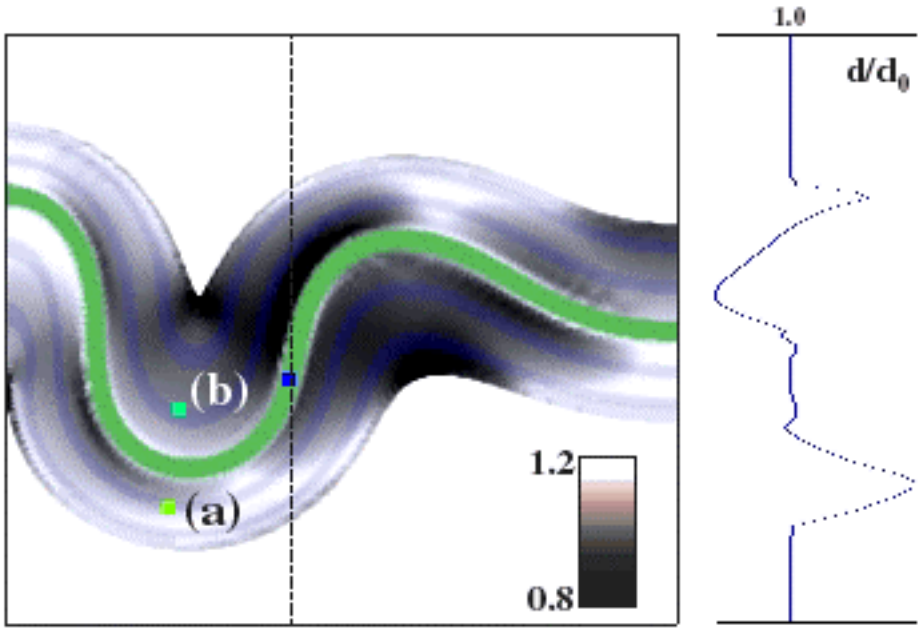

Figure 22: As Figure 19, but now the rheology is sensitive to grain size. The pattern of grain size variation is more complicated in this picture, but the magnitude of the variations is smaller than in Figure 19.

Figure 22 shows a snapshot of the deformation pattern at 44% axial shortening, but this time assuming a grain size dependence for the rheology $m^{(2)}=3$. The grain size dependence of the viscosity (de)stabilizes the deformation since the viscosity is smallest where, according to (9), the stress is highest. This grain-softening effect is clearly reflected in the more localized and discontinuous appearance of the grain-size pattern in Figure 22 compared to that in Figure 19. Grain size histories for this case are very similar to those shown in Figure 20, however, the magnitude of grain size variations and stresses is moderated by the softening effects.

The plasticity like appearance of the fold deformation field is not entirely surprising. If the fold amplitudes evolve on a much larger time scale than the relaxation time of grain growth we may write $d/d_0 = d_\infty/d_0 = B(\tau/\tau_0)^{-p}$; insertion into

$$\tau = \eta_0 \left(\frac{d}{d_0}\right)^m \dot{\gamma} \qquad (11)$$

and rearranging gives

$$\tau = \tau_0 \left(\frac{\eta_0}{\tau_0} B^m \dot{\gamma}\right)^{\frac{1}{(mp+1)}} \qquad (12)$$

which is formally identical to the power law relationships of dislocation creep. In our finite element calculations we have tacitly treated grains as material objects which they are not.

The local equilibrium value of the average grain diameter is determined among other things by strain energy or the energy of stress or strain fluctuations, it is not so clear at the grain scale

(eg den Brok *et al*., 1999). Grain boundaries seem to migrate on the microscopic scale towards local stress concentrations or equivalently towards zones of elastic strain energy concentrations. Phenomenological relationships such as (8) and (9) apply in such cases provided that the fluctuation energy is scaled by some global stress measure and that stress or strain energy gradients are not significant on the scale at which we apply our continuum description. If macroscopic stress gradients are present then we have to expect, at least in principle, a drift of the centres of the average grains of our model against the stress gradient towards zones of high stresses.

Such ideas may be incorporated into a more refined model for the dynamics of evolving grains by first introducing a grain number density ν as

$$\nu \frac{1}{6} \pi d_0 \left(\frac{d}{d_0} \right)^3 = \varphi_g \qquad (13)$$

where $\varphi_g \approx 1$ is the volume fraction occupied by grains. The rate of ν may be written as

$$\dot{\nu} = \nu_{,t} + (v_i + \bar{v}_i) \frac{f\nu}{fx_i} \qquad (14)$$

where $\bar{v}_i$ is the relative drift velocity of the grain centres. Following the idea that grain boundaries migrate up the stress gradient we may assume for the case of microscopic isotropy

$$\bar{v}_i = \vartheta \frac{\partial \rho e}{\partial x_i} \qquad (15)$$

where $\vartheta(1/RT, d, ...)$ is a phenomenological coefficient and $\rho e(\tau, p)$ is the elastic strain energy per unit volume. The influence of grain centre drift on the evolution of the spatial distribution of average grain sizes will be explored in more detail in a forthcoming paper.

At this stage it is understood however that the above energy gradient relationship is speculative and more experimental work is required to substantiate such a relationship.

6. DISCUSSION AND CONCLUSIONS

The classical work of Biot (1957, 1965) and of Ramberg (1963) has had a profound influence on the way we think about the mechanics of folding. Even though these treatments are small amplitude, two dimensional, linear theories, they highlight the essential characteristics of all subsequent, more elaborate theories. The essential characteristics here are, given adequate contrasts in constitutive parameters between a layer and its embedding medium, a wavelength selection process begins operating early in the deformation process; eventually a critical wavelength is amplified at an exponential rate to form strictly periodic waveforms independent of initial geometrical irregularities (unless, of course, these initial geometrical irregularities happen to have a wavelength coincident with that of the critical wavelength which is preferentially amplified).

As more complicated constitutive relationships have been investigated in recent years and as more general (large amplitude) and three dimensional theoretical treatments have been developed, it appears that modifications to the Biot/Ramberg linear theories arise:

(i) For viscous, non-linear (specifically, power law) materials, the critical wavelength which is amplified is less than that predicted for a linear-viscous material; for instance, if the power law exponent in the stress-strain rate relation is 0.5 then the wavelength amplified is 0.8 of that expected by the Biot theory with the viscosity defined by (6).

(ii) For purely viscous materials deforming in three dimensions, two wavelengths are always amplified no matter if the deformation history is biaxial shortening, plane shortening or shortening plus extension in the plane of the layer. These two wavelengths combine to give the impression of superimposed fold systems; in a particular section plane through the fold system this may result in fold system profiles that are a-periodic.

(iii) Combining linear elastic behaviour with viscous behaviour immediately introduces the possibility that parasitic folds will develop. Hence, in two dimensions, we have the possibility of fold systems characterised by two dominant wavelengths and not just one as in the classical theories.

(iv) Elastoviscous materials undergo a spectrum of responses ranging from the domination of homogeneous shortening and weak buckling at relatively low strain rates, to little layer parallel shortening and predominantly buckling deformation at relatively high strain rates (for a given set of physical parameters).

The position in this spectrum of behaviour is governed by the Deborah Number which expresses the balance between the time scale for amplification of the fold system and the time scale for viscous relaxation of the system. For Deborah Numbers less than one, homogeneous shortening dominates with the result that initial geometrical irregularities are mainly passively amplified and have a dominating influence on the final shapes of deformation features. In some situations (eg. a favourable wavelength) the dynamic fold growth rate may become

significant in later deformation stages. However, the wavelength selection mechanism which generates the Biot type wavelength is still not possible here because the limb dips of initial perturbations can reach quite high angles into finite amplitude fields during early homogeneous shortening and passive growth stages. Then initial geometrical irregularities again control final fold shapes. For Deborah Numbers greater than one, a Biot type wavelength selection process dominates over layer parallel shortening and deformation characterised by dynamic buckling dominates. In such a process initial geometrical irregularities are "de-amplified" so that initial geometrical irregularities play a minor role in governing final fold shapes. Since there is a strong relationship between viscosity, elastic moduli, competency contrast and the stress induced by a given imposed strain rate, the generalisations mentioned above depend intrinsically upon where one is in viscosity, elastic moduli, competency contrast, strain rate space.

(v) The consideration of higher forms of non-linearity in the constitutive relations leads to even more complicated geometrical response. Specifically, the introduction of elastic softening into the simple Maxwell elastoviscous material behaviour results in the development of localised packages of folds within a layer rather than the infinitely extended periodic waveform predicted by the classical Biot/Ramberg theories. These localised packages of deformation have a distinctly fractal spatial distribution, the position and precise geometry of the localised fold package being critically dependent upon the initial kinematic framework. This kind of behaviour has all the hallmarks of a chaotic dynamic system.

(vi) Particle-in-cell finite element simulations of grain growth evolution during folding demonstrate the possibility that we may be able to map more accurately the deformation history by incorporating detailed information about relative grain growth rates and deformation rates. Grain size variation under applied stress leads to an additional softening mechanism which, in the limit of fast recrystallization, produces a simple power-law rheology, but which, in the case of recrystallization at rates comparable to deformation, would produce a more general behaviour where history dependent rheology influences the deformation itself.

REFERENCES

Abbassi, M.R. & Mancktelow, N.S. 1990. The effect of initial perturbation shape and symmetry on fold development. *J. Struct. Geol.* **12**, 273-282.

Abbassi, M.R. & Mancktelow, N.S. 1992. Single layer buckle folding in non-linear materials – I. Experimental study of fold development from an isolated initial perturbation. *J.Struct. Geol.* **14**, 85-104.

Biot, M.A. 1937. Bending of an infinite beam on an elastic foundation. *ASME J. Appl. Mech.* **A59**, 1-7.

Biot, M.A. 1957. Folding instability of a layered viscoelastic medium under compression. *Proc. R. Soc. Lond.* **A242**, 111-454.

Biot, M.A. 1959. On the instability of folding deformation of a layered viscoelastic medium in compression. *J. Appl. Mech.* **26**, 393-400.

Biot, M.A. 1961. Theory of folding of stratified viscoelastic media and its implications in tectonics and orogenesis. *Geol. Soc. Am. Bull.* **72**, 1595-1620.

Biot, M.A. 1963. Internal buckling under initial stress in finite elasticity. *Proc. Royal Soc.* **A273**, 306-328.

Biot, M.A. 1965. *Mechanics of Incremental Deformations.* John Wiley, New York. 504pp.

Bons, P. D., Jessell, M. W., and Brecht, G. 1997. Domain boundary migration in experiment and nature, http://www.earth.monash.edu/~mark/history/history.html

Braun, J. Chery, J. Poliakov, A. Mainprice, D. Vauchez, A. Tomassi, A. & Daignieres, M. 1999. A simple parameterization of strain localization in the ductile regime. Submitted to *J. Geophys. Res.*

Budd, C.J. Hunt, G.W. & Peletier, M.A. 1998. Self-similar fold evolution under prescribed end-shortening. *Technical report 98-13*, University of Bath.

Budd, C.J. & Peletier, M.A. 1998. Approximate self-similarity in models of geological folding. *Technical report 98-09*, University of Bath.

Chapple, W.M. 1969. Fold shape and rheology: the folding of an isolated viscous-plastic layer. *Tectonophysics*. **7**, 97-116.

Cobbold, P.R. 1975. Fold propagation in single embedded layers. *Tectonophysics*. **27**, 333-351.

Cobbold, P.R. 1977. Finite-element analysis of fold propatation – a problematic application? *Tectonophysics*. **38**, 339-353.

Crutchfield, J.P. Farmer, J.D. Packard, N.H. & Shaw, R.S. 1986. Chaos. *Scientific American* **255 (6)**, 38-49.

Den Brok B, Zahid M, Passchier C.W. 1999. Stress induced grain boundary migration in very soluble brittle salt, **21**, 147-151

Derby, B. & Ashby, M.F. 1987. On dynamic recrystallisation, *Seripta Metall*. **21**, 879-884.

Fletcher, R.C. 1974. Wavelength selection in the folding of a single layer with power-law rheology. *Am. J. Sci.* **274**, 1029-1043.

Fletcher, R.C. 1991. Three-dimensional folding of an embedded viscous layer in pure shear, *J. Struct. Geol.*, **13**, 87-96.

Frost, H. J. and Ashby, M. F., 1982 Deformation Mechanism Maps, Pergamon, Oxford.

Ghosh, S.K. 1970. A theoretical study of intersecting fold patterns. *Tectonophysics*. **9**, 559-569.

Holmes, P. 1990. Nonlinear dynamics, chaos, and mechanics. *Appl. Mech. Rev.* **43**, S23-S39.

Hudleston, P.J. 1973. An analysis of "single-layer" folds developed experimentally in viscous media. *Tectonophysics* **16**, 189-214.

Hudleston, P.J. & Lan, L. 1994. Rheological controls on the shapes of single-layer folds. *J. Struct. Geol.* **16**, 1007-1021.

Hunt, G.W. & Lawther, R. 1999. Finite element modelling of spatially-chaotic structures. In press.

Hunt, G.W. Mühlhaus, H.-B. & Whiting, A.I.M. 1996a. Evolution of localized folding for a thin elastic layer in a softening visco-elastic medium. *Pure Appl. Geophys*. **146**, 229-252.

Hunt, G.W. Mühlhaus, H.-B. Hobbs, B. & Ord, A. 1996b. Localized folding of viscous layers. *Geologische Rundschau (Int. J. Earth Sciences)* **85**, 58-64.

Hunt, G.W. Mühlhaus, H.-B. & Whiting, A.I.M. 1997. Folding processes and solitary waves in structural geology. *Phil. Trans. R. Soc. Lond.* A **355**, 2197-2213.

Hunt, G.W. Wadee, M.K. & Shiacolas, N. 1993. Localized elasticae for the strut on the linear foundation. *J. Appl. Mech*. **60**, 1033-1038.

Jaeger, J.C. 1969. *Elasticity, Fracture and Flow.* Methuen & Co. Ltd, London. 268pp.

Johnson, A.M. & Fletcher, R.C. 1994. *Folding of Viscous Layers.* Columbia University Press. 461pp.

Kameyama, M. Yuen, D.A. & Fujimoto, H. 1997. The ineraction of viscous heating with grain-size dependent rheology in the formation of localized slip zones. *Geophys. Res. Lett*. **24**, 2523-2526.

Karato, S. Paterson, M.S. & FitzGerald, J.D. 1986. Rheology of synthetic olivine aggregates: influence of grain size and water. *J. Geophys. Res*. **91**, 8151-8176.

Karato, S.-I., and Wu, P., 1993 Rheology of the upper mantle: A synthesis, Science, 260, 771-778.

Lan, L.& Hudleston, P.J. 1991. Finite element models of buckle folds in non-linear materials. *Tectonophysics* **199**, 1-12.

Mancktelow, N.S. & Abbassi, M.R. 1992. Single layer buckle folding in non-linear materials – II. Comparison between theory and experiment. *J. Struct. Geol.* **14**, 105-120.

Mancktelow, N.S. 1999. Finite-element modelling of single-layer folding in elasto-viscous materials: the effect of initial perturbation geometry. *J. Struct. Geol*. (in press).

Mayer-Kress, G. & Kaneko, K. 1989. Spatiotemporal chaos and noise. *J. Stat. Phys.* **54**, 1489-1508.

Moresi, L., Gurnis, M., Zhong, S. 2000. Plate tectonics and convection in the Earth's mantle: toward a numerical simulation, Computing in Science and Engineering, **2**, 22-33.

Mühlhaus, H.-B., Moresi, L., Sakaguchi, H., 2000. Discrete and continuum modelling of granular materials, in *Constitutive Modelling of Granular Materials* (edited by Kolymbas, D.) Springer, pp 209-224.

Mühlhaus, H.-B. 1993. Evolution of elastic folds in plane strain. In: *Modern Approaches to Plasticity* (edited by Kolymbas, D.). Elsevier, New York. 734-765.

Mühlhaus, H.-B. Sakaguchi, H. & Hobbs, B.E. 1998. Evolution of three-dimensional folds for a non-Newtonian plate in a viscous medium. *Proc. R. Soc. Lond. A* **454**, 3121-3143.

Ord, A. 1992. The fractal geometry of patterned structures in numerical models of rock deformation. In: *Fractals and Dynamic Systems in Geoscience* (edited by J.H. Kruhl). Springer, Berlin, Heidelberg, New York. 223-231.

Packard, N.H. Crutchfield, J.P. Farmer, J.D. & Shaw, R.S. 1980. Geometry from a time series. *Phys. Rev. Lett.* **45**, 712-716.

Price, N.J. & Cosgrove, J.M. 1990. *Analysis of Geological Structures*. Cambridge University Press, Cambridge.

Ramberg, H. 1963. Fluid dynamics of viscous folding. *Am. Assoc. Petrol. Geol. Bull*. **47**, 484-515.

Ruelle, D. 1990. Deterministic chaos: the science and the fiction. The Claude Bernard Lecture, 1989. *Proc. R. Soc. Lond*. **A427**, 241-248.

Sander, B. 1930. *Gefügekunde der gesteine.* Julius Springer, Vienna. 352pp.

Smith, R.B. 1977. Formation of folds, boudinage and mullions in non-Newtonian materials. *Bull. Geol. Soc. Am.* **88**, 312-320.

Smith, R.B. 1979. The folding of a strongly non-Newtonian layer. *Am. J. Sci.* **279**, 272-287.

Takens, F. 1981. Detecting strange attractors in turbulence. In: *Dynamical systems and Turbulence* (edited by Rand, D.A. & Young, L.S.). *Lecture Notes in Mathematics* **898**, 366-381.

Treagus, S. H. 1973. Buckling stability of a viscous single-layer system oblique to the principal compression. *Tectonophysics* **19**, 271-289.

Whiting, A.I.M. & Hunt, G.W. 1997. Evolution of nonperiodic forms in geological folds. *Math. Geol.* **29**, 705-723.

Williams, J.R. Lewis, R.W. & Zienkiewicz, O.C. 1978. A finite-element analysis of the role of initial perturbations in the folding of a single viscous layer. *Tectonophysics* **45**, 187-200.

Willis, B. 1893. The mechanics of Appalachian structures. *United States Geological Survey 13th Annual Report*, 211-281.

Zhang, Y. Hobbs, B.E. Ord, A. & Mühlhaus, H.-B. 1996. Computer simulation of single layer buckling. *J. Struct. Geol.* **18**, 643-655.

Zhang, Y. Hobbs, B.E. Ord, A. & Mühlhaus, H.-B. 1999a. What controls fold shape? Clarification of an issue regarding the influence of initial irregularities. Submitted to *J. Struct. Geol.*

Zhang, Y. Hobbs, B.E. Ord, A. & Mühlhaus, H.-B. 1999b. A clarification of an issue regarding the influence of initial irregularities upon fold shape. In: Abstract volume of Last Conference of the Millenium – The Specialist Group in Tectonics and Structural Geology Conference (Halls Gap, Victoria, Australia), *GSA Abstracts Series* **53**, 278-279.

Zhang, Y. Hobbs, B.E. Ord, A. & Mühlhaus, H.-B. 1999c. Folding of viscoelastic materials. In preparation.

Zhang, Y. Mancktelow, N.S. Hobbs, B.E. Ord, A. and Mühlhaus, H.-B. 2000. Numerical modelling of single-layer folding: clarification of an issue regarding the effect of computer codes and the influence of initial irregularities. *J. Struct. Geol.* (in press).